HAL
open science

Effect of local and regional oceanographic processes on the recovery of macroalgal communities post-El Niño in the rocky intertidal along the Oregon coast

Camille Ollier

To cite this version:

Camille Ollier. Effect of local and regional oceanographic processes on the recovery of macroalgal communities post-El Niño in the rocky intertidal along the Oregon coast. Life Sciences [q-bio]. 2018. dumas-01971662

HAL Id: dumas-01971662

https://dumas.ccsd.cnrs.fr/dumas-01971662v1

Submitted on 7 Jan 2019

HAL is a multi-disciplinary open access archive for the deposit and dissemination of scientific research documents, whether they are published or not. The documents may come from teaching and research institutions in France or abroad, or from public or private research centers.

L'archive ouverte pluridisciplinaire **HAL**, est destinée au dépôt et à la diffusion de documents scientifiques de niveau recherche, publiés ou non, émanant des établissements d'enseignement et de recherche français ou étrangers, des laboratoires publics ou privés.

AGROCAMPUS OUEST

☐ **CFR Angers**

☑ **CFR Rennes**

Année universitaire : 2017-2018

Spécialité : Ingénieur Agronome

Spécialisation (et option éventuelle) :

Sciences halieutiques et aquacoles

(Option REA)

Mémoire de Fin d'Études

☑ d'Ingénieur de l'Institut Supérieur des Sciences agronomiques, agroalimentaires, horticoles et du paysage

☐ de Master de l'Institut Supérieur des Sciences agronomiques, agroalimentaires, horticoles et du paysage

☐ d'un autre établissement (étudiant arrivé en M2)

Effect of local and regional oceanographic processes on the recovery of macroalgal communities post-El Niño in the rocky intertidal along the Oregon coast

Par : Camille OLLIER

Soutenu à Rennes, le 13/09/2018

Devant le jury composé de :

Président : Olivier LE PAPE

Maître de stage : Bruce MENGE et Barbara SPIECKER

Enseignant référent : Olivier LE PAPE

Autres membres du jury

Manuel PLANTEGENEST (Chercheur ACO Rennes)

Martial LAURANS (Chercheur Ifremer Brest)

Les analyses et les conclusions de ce travail d'étudiant n'engagent que la responsabilité de son auteur et non celle d'AGROCAMPUS OUEST

Ce document est soumis aux conditions d'utilisation
«Paternité-Pas d'Utilisation Commerciale-Pas de Modification 4.0 France»
disponible en ligne http://creativecommons.org/licenses/by-nc-nd/4.0/deed.fr

Confidentialité

☑ Non ☐ Oui si oui : ☐ 1 an ☐ 5 ans ☐ 10 ans

Pendant toute la durée de confidentialité, aucune diffusion du mémoire n'est possible [1].

Date et signature du **maître de stage** [2] :
(ou de l'étudiant-entrepreneur) 30/08/2018

A la fin de la période de confidentialité, sa diffusion est soumise aux règles ci-dessous (droits d'auteur et autorisation de diffusion par l'enseignant à renseigner).

Droits d'auteur

L'auteur[3] **OLLIER Camille**
autorise la diffusion de son travail (immédiatement ou à la fin de la période de confidentialité)

☑ Oui ☐ Non

Si oui, il autorise

☐ la diffusion papier du mémoire uniquement(4)

☐ la diffusion papier du mémoire et la diffusion électronique du résumé

☑ la diffusion papier et électronique du mémoire (joindre dans ce cas la fiche de conformité du mémoire numérique et le contrat de diffusion)

(Facultatif) ☐ accepte de placer son mémoire sous licence Creative commons CC-By-Nc-Nd (voir Guide du mémoire Chap 1.4 page 6)

Date et signature de l'**auteur** :
30/08/2018

Autorisation de diffusion par le responsable de spécialisation ou son représentant

L'enseignant juge le mémoire de qualité suffisante pour être diffusé (immédiatement ou à la fin de la période de confidentialité)

☐ Oui ☐ Non

Si non, seul le titre du mémoire apparaîtra dans les bases de données.
Si oui, il autorise

☐ la diffusion papier du mémoire uniquement(4)

☐ la diffusion papier du mémoire et la diffusion électronique du résumé

☐ la diffusion papier et électronique du mémoire

Date et signature de l'**enseignant** :

(1) L'administration, les enseignants et les différents services de documentation d'AGROCAMPUS OUEST s'engagent à respecter cette confidentialité.
(2) Signature et cachet de l'organisme
(3).Auteur = étudiant qui réalise son mémoire de fin d'études
(4) La référence bibliographique (= Nom de l'auteur, titre du mémoire, année de soutenance, diplôme, spécialité et spécialisation/Option)) sera signalée dans les bases de données documentaires sans le résumé

Acknowledgments

Undertaking this Master's internship has been a truly life-changing experience for me and it would not have been possible without the support and guidance of many people. First and foremost, I would like to say a very big thank you to my fantastic supervisors Bruce Menge and Barbara Spiecker for all their guidance, encouragement and patience. I had a lot of fun sharing this 6-month internship with you both scientifically and personally. I would also like to thank Barbara Spiecker for your support and your valuable advice for my future career.

I am thankful for the guidance and the financial support from two associations: Bourse de Thomas Dricot and Jeunes à Travers le Monde.

I am also ever so grateful for the support from so many highly talented individuals including Brittany Poirson, Jenna Sullivan, Sarah Gravem, Jonathan Robinson and many others. They made fieldwork more memorable than ever.

I would also thank all my interpreters in France (whose presence I required and strived to get across my academic years) and in the United States. Without them, I would not have had equal learning opportunity.

I would also like to say a personal thank you to my family, friends and roommates. Their supports are unmeasurable, and this journey to the degree would have been far more difficult without them. In particular, I thank my mother – whose dreams for me resulted in this achievement. Without her support, I would not have been where I am today and what I am today.

Résumé

Contexte et objectifs

Les communautés marines sont connues pour être affectées par l'approvisionnement ascendant des nutriments et autres ressources vitales. La disponibilité de ces ressources est souvent dictée par les conditions environnementales locales. Le changement climatique mondial pourra modifier certaines communautés.

L'upwelling un des processus fondamentaux de l'océan se produit lorsque les vents du large repoussent les eaux de surface chaudes de la côte et permettent à l'eau profonde, froide et riche en nutriments, de remonter vers la surface. Ces zones d'upwelling sont présentes dans plusieurs endroits du globe terrestre et quatre d'entre elles sont parmi les zones marines les plus productives (Californie, Canaries, Humboldt et Benguela). Ces systèmes d'upwelling mondiaux des marges océaniques orientales apportent 7 % de la production primaire mondiale et plus de 20 % des captures mondiales de poissons marins.

Des phénomènes affectent tel que El Niño viennent perturber les zones d'upwelling. Ce phénomène correspond à un inversement des vents de surface et donc un changement dans les températures de l'eau (créant généralement une hausse de température de l'eau et réduisant l'impact des upwellings). Ce phénomène est couplé à un autre appelé la Niña et à eux deux ils forment le phénomène ENSO (*El Niño-Southern Oscillation)*.

Le varech, une macro-algue brune non calcifiée, a été identifié comme espèce clé pour maintenir le fonctionnement de l'écosystème. Cette famille d'algue peut être affectée par le phénomène ENSO.

La zone d'étude située sur la côte de l'Oregon est une zone soumise à ce phénomène d'upwelling. De nombreuses espèces de varech sont présentes sur ces côtes et peuvent être impactées par le phénomène El Niño. Une étude a été réalisé en 1998-2000 par Freindeinburg sur les communautés algales sur la côte de l'Oregon après le phénomène El Niño en 1997-98. L'étude portait sur les réponses à court terme des communautés algales face au phénomène El Niño. Une des hypothèses étudiées était que l'upwelling pouvait continuer à apporter les nutriments nécessaires au développement des algues malgré le réchauffement des eaux dû à El Niño. L'étude de l'abondance et de la croissance du varech présent dans les zones intertidales de la côte de l'Oregon a été réalisé pour établir l'impact de l'upwelling et d'El Niño sur les communautés algales. Avec quelques observations des différences régionales sur l'abondance et la croissance du varech intertidal, l'hypothèse a été établie que la variation spatiale peut être modifiée par l'upwelling côtier.

Le projet de recherche s'articule autour de l'étude de l'impact du phénomène El Niño sur l'abondance et la croissance des algues brunes suite à l'épisode de 2015-2016. Le but d'examiner la manière dont les processus environnementaux locaux et régionaux modulent les effets d'El Niño sur les communautés de varech le long de la côte de l'Oregon.

Matériel et méthodes

Trois espèces de varech ont été étudié. *Postelsia palmaeformis, Egregia menziesii* et *Saccharina sessilis.* Ce sont des espèces de macroalgues intertidales communes du genre Laminaria. Chaque mois, les caractéristiques démographiques étudiées avec la méthode des transects. Leur pourcentage de couverture, leur densité et leur croissance ont été mesurés à l'aide d'un quadrat de 0,25 m^2 placé de manière contiguë des deux côtés du transect, soit un total de 20 quadrats par transect.

Les paramètres environnementaux pouvant avoir un impact sur ces communautés algales ont aussi été étudiés. L'indice d'action de la vague (hauteur de la vague), l'upwelling, l'indice Multivarié ENSO (variations associées aux phénomènes El Niño et

La Niña), l'oscillation décennale du Pacifique, le Gyre subtropical du Pacifique nord, les concentrations de chlorophylle et de nutriments ainsi que la température de surface de l'eau sont les paramètres environnementaux qui ont été analysés en lien avec les caractéristiques démographiques des algues. Ces données sont tirées des bases de données de la NOAA et d'autres organismes de recherche. Elles ont été traitées (moyennées) pour pouvoir être utilisées dans l'analyse. Les données entre 2016 et 2018 ont été analysées.

L'analyse statistique des résultats a été réalisée à l'aide d'un modèle à effets mixtes pour tester la réponse biologique (pourcentage de couverture et longueur de l'algue). Les facteurs « année », « mois », et le lieu de prélèvement ont été considérés comme des facteurs fixes à cause de l'intérêt direct qu'ils avaient sur l'étude. Les facteurs « transect » et « quadrat » ont été considérés comme des facteurs aléatoires. Les modèles réalisés au final pour chaque espèce ont été réalisés en enlevant des facteurs d'un modèle complet basé sur le critère d'information d'Akaike (AIC).

Résultats

Les résultats ont montré que les processus environnementaux locaux et régionaux modulent bel et bien la force d'El Niño et ses effets sur la restauration des communautés de varech le long de la côte de l'Oregon. Il y a une différence marquée dans les trajectoires de récupération des macroalgues intertidales le long de la côte de l'Oregon après El Niño en 2015-2016. L'abondance et la taille du varech intertidal ont été réduites par l'événement El Niño de 2015-2016 et ont montré une tendance générale à l'augmentation de l'abondance entre 2016 et 2018, avec un fort taux de récupération la première année. Les réponses régionales de *Saccharina* et *Postelsia* peuvent être expliquées par des différences dans la topographie côtière et les processus océanographiques.

En effet, l'upwelling côtier dans la région sud, se produit plus fréquemment que dans les régions du centre et du nord. Par conséquent, les algues intertidales dans le sud ont davantage accès aux nutriments et pourraient expliquer pourquoi elles se rétablissent. Cependant, la dépression de la thermocline pourrait découpler le système de nutriments du courant ascendant, car l'upwelling apporte des eaux plus chaudes et appauvries en nutriments. Le sud de l'Oregon pourrait fournir de refuge au varech en raison du fort gradient d'upwelling, mais la force des changements temporels à grande échelle peut l'emporter sur les différences régionales, rendant ainsi le refuge localisé inhospitalier. Les changements climatiques pourraient ne pas modifier la fréquence et l'intensité de la remontée des eaux côtières dans le système californien actuel, mais ils pourraient modifier la chimie de l'upwelling ; de ce fait, le changement climatique pourrait contribuer à l'intensification d'El Niño à plus grande échelle avec des tempêtes persistantes et violentes. Dans le Pacifique tropical, la durée totale de l'El Niño 2015-2016 a été supérieure à celui de 1997-98. Les tempêtes renforcées par El Niño et le changement climatique, ajoutées à la stratification des océans et des eaux chaudes et appauvries en nutriments produites par les remontées d'eau, pourraient avoir des conséquences graves et durables sur les communautés de varech importantes, tant d'un point de vue écologique qu'économique. Les liens entre le changement climatique et les signaux océanographiques tels qu'El Niño — Oscillation Sud et l'upwelling côtier restent incertains.

Conclusion

Cette recherche montre que les processus locaux et régionaux modulent la force d'El Niño sur les communautés de varech intertidales. Les résultats suggèrent la possibilité que la remontée d'eau soit une arme à double tranchant face aux processus climatiques persistants à grande échelle (ex. : le réchauffement). Elle pourrait impliquer la mutation des relations bénéfiques entre les remontées d'eau et les communautés de varech en une relation néfaste. Afin de mieux comprendre et anticiper les ramifications futures du changement climatique sur les communautés de varech intertidales, une analyse plus approfondie de la physiologie du varech est nécessaire pour expliquer en quoi les varechs diffèrent dans leurs réponses aux divers facteurs environnementaux. En outre, l'étude devrait être menée à des échelles spatiales et temporelles plus grandes afin de quantifier les liens entre les facteurs climatiques tels qu'El Niño et les communautés biologiques.

Abstract

Although the links between climate change and climatic patterns such as ENSO (El Niño-Southern Oscillation) remain unclear, the impacts of ENSO events on coastal environments in the short-term likely mimic those of climate change in the long-term. Thus, ENSO can serve as a proxy for possible long-term ecological responses to an increasingly variable climate. ENSO events can have dramatic effects on species interactions and the structuring of communities. However, the impact of El Niño could be modulated by local and regional processes (i.e., nutrient inputs from upwelling and coastal topography). The Oregon rocky intertidal is exposed to a gradient of upwelling from weaker and intermediate (northern Oregon) to stronger and more persistent (southern Oregon) and the coastal topography varies from site to site. The results showed that local and regional environmental processes do modulate the strength of El Niño and its effects on the recovery of kelp communities along the Oregon coast. Intertidal kelp abundance and size were reduced by the 2015-16 El Niño event (more so in the southern Oregon) and they were recovered two years after the event with a faster recovery rate in the southern Oregon. The results hint at the possibility of persistent large-scale climatic processes (i.e., warming) shifting the beneficial relationship between upwelling and kelp communities to a harmful one. More research is needed on larger spatial and temporal scales to better understand and anticipate future climate change ramifications on the intertidal kelp communities.

List of Acronyms

BB: Boiler Bay
CB: Cape Blanco
CBN: Cape Blanco North
CF: Cape Foulweather
CP: Cape Perpetua
DB: Depoe Bay
DIN: Dissolved Inorganic Nitrogen
ENSO: El Niño – Southern Oscillation
ESMs: Environmental stress models
FC: Fogarty Creek
MEI: Multivariate ENSO Index
NPGO: North Pacific Gyre Oscillation
N/PMs: Nutrient/productivity models
NOAA: National Oceanic and Atmospheric Administration
PDO: Pacific Decadal Oscillation
PISCO: Partnership for Interdisciplinary Studies of Coastal Oceans
SH: Strawberry Hill
SST: Sea Surface Temperature
SWVHT: Significant Wave Height
RP: Rocky Point
YB: Yachats Beach

Table of contents

1. Introduction 1
2. Methods 4
2.1 Study area 4
2.2 Time Span 5
2.3 Overview of study organisms 5
2.4 Quantification of macroalgae communities 7
2.5 Environmental parameters 8
2.5.1 At meso-scale 8
2.5.2 At macro-scale 9
2.5.3 Data frame 10
2.6 Data analysis 10
3. Results 11
3.1 Spatiotemporal responses of three common intertidal macroalgae 11
3.1.1 Saccharina sessilis 11
3.1.2 Egregia menziesii 12
3.1.3 Postelsia palmaeformis 13
3.2 Seasonal variability 14
3.3 Environmental factors 15
3.4 Local and regional spatial variability of distribution of Saccharina sessilis 17
3.5 Comparison with Freidenburg's papers 17
4. Discussion 19
5. Conclusion 21

1. Introduction

Climate Change, Upwelling and El Niño

It is well known that communities are strongly affected by bottom-up supply of nutrients and other vital resources (Menge, 2000). The availability of these resources is often dictated by local environmental conditions. Global climate change is predicted to fundamentally alter a variety of environmental conditions, including one of the ocean's fundamental processes: upwelling. At mid-latitudes, the surface layer produces a stratification which prevents cool, nutrient-rich deep water from mixing with the warm surface water and causes a nutrient limitation to primary production at the surface. Upwelling occurs when coastal winds push warm surface waters away from the shore and allow deep, cold, nutrient-rich water to rise toward the surface. This oceanographic process is present in many parts of the world. Eastern Boundary Upwelling Systems, consisting of four upwelling zones, are among the most productive marine areas in the world (Bakun et al., 2015). The Eastern Boundary current systems cover less than 2% of the ocean surface but provide 7% of global primary production and more than 20% of global fish catches (Xiu et al., 2018). Large-scale climate-driven biological variability such as the El Niño Southern Oscillation (ENSO) causes strong interannual and interdecadal climate variability on the coastal upwelling ecosystems (Barber, 2008). The oscillation includes El Niño and La Niña events, which alternate every 3–5 years. El Niño is the warm period of the ENSO cycle. In addition to the rise in sea surface temperature, climate models predict El Niño events will increase in intensity and frequency. One of the features of El Niño is increased winter storms and elevated wave actions, which can lead to loss of habitat and ecological (Wernberg et al., 2010). But the future of upwelling under anthropogenic climate change remains unclear. The Bakun hypothesis revealed that global warming drives intensification of winds and leads to upwelling favorable winds due to a cross-shore pressure gradient intensifying upwelling (Bakun et al., 2015; Sydeman et al., 2014). Models showed that the Bakun hypothesis is validated at high latitude and the trend in upwelling intensity and duration decreased when the latitude is low (Wang et al., 2015). Previous models showed that increased land-sea temperature and upwelling intensification is correlated in three of the Eastern Boundary Upwelling Systems (Canary, Benguela and Humboldt) (Wang et al., 2015). Despite the intensification of upwelling with global warming, Wang et al. (2015) suggested that the California current system (CalCS) will not show upwelling intensification due to the strong influences of ENSO, the Pacific Decadal Oscillation (PDO) and the North Pacific Gyre Oscillation (NPGO). These oceanography processes modulate winds patterns and could impact the upwelling distribution in CalCS.

Scientists have suggested various approaches to determining the consequences of coastal upwelling under the influence of El Niño. Benthic bacteria use up oxygen and release carbon dioxide, which causes deep seawater to have very low oxygen. The nutrient-rich upwelled waters are essential to keep the coastal marine ecosystem healthy and productive, but hypoxic (oxygen-depleted) waters can have negative consequences (Bakun et al., 2015). Therefore, Wang et al. (2015) established that increased persistent upwelling due to climate change is decoupled from the supply of nutrient rich water and is a threat to the marine ecosystem. On another hand, Wang and colleagues (2015) explained that the increased upper-ocean stratification with global warming could lead to upwelling circulation that is warm and depleted of nutrients, and an increase in global hypoxia. The physical process of upwelling continues during ENSO events, but in contrary the chemistry of the water is dramatically changed (Barber, 2008) and causes primary production reduction.

The future of upwelling under anthropogenic climate change remains unclear and its effects on marine ecosystems are not easy to predict. The importance of understanding the impacts of El Niño on marine ecosystems motivated my research on the Oregon coast. Patterns

on the coast of Oregon suggest that community structure be based both on small-scale (i.e. species interactions, waves forces, thermal/desiccation gradients) and larger-scale processes (i.e. nutrient availability, phytoplankton productivity, detritus and larval transport). In addition, research shows that the effects of nutrient addition during La Niña conditions on the Oregon coast lead to spatial variation in algal responses (Freidenburg et al., unpublished thesis chapter, 2002; Menge, 2000). Cape Foulweather, the most northern area, is exposed to weaker, intermittent upwelling as compared to Cape Blanco, the most southern area which has stronger and more persistent upwelling. This natural spatial variation in physical characteristics and biological communities makes the Oregon coast an optimal area to study the responses of species in response to oceanographic processes.

Kelp as an Ecological and Economic Resource

Kelp, an order of brown non-calcified macroalgae, has been identified as a foundation species which plays an important role in ecosystem functioning (Dayton, 1985). By modifying both the physical conditions and as a primary producer, kelp has a disproportionate influence on its community. Kelp stabilizes conditions for other associated species (Falkenberg et al., 2012). Kelp in the open coast rocky intertidal zone is especially important because it is adapted to withstand large wave forces, and subsequently provide protected habitat for other species. Kelp also interacts with a multitude of species by providing food for grazers, which indirectly benefits many other species. On a larger scale, kelp plays an important role by helping to reduce atmospheric carbon dioxide concentrations. Its capacity to absorb CO_2 could reach twelves times as much as the amount from the atmosphere (Wilmers C. et al., 2012). Thus, kelp helps prevent elevated ocean acidification, which threatens the marine environment. Kelp also provides an important value to the economy. The seaweed industry has an estimated total annual value of $6 billion (McHugh, FAO, 2003). Seaweeds are used as animal and human food as well as fertilizers. Extracted substances from microalgae are used frequently in the food industry, cosmetics, pharmaceutical industry, and biotechnology. In the future, aquaculture of kelp will likely intensify, especially as a food source and in integrated multi-trophic aquaculture systems.

Kelps are increasingly threatened by a diversity of stressors on multiple scales. First, coastal marine ecosystems are increasingly affected by anthropogenic pressures like harvesting, pollution, and invasive species. Kelp is a cold-water species and is vulnerable to a wide range of disturbances such as temperature stress, wave disturbance and overgrazing by sea urchins (Byrnes et al., 2011; Krumhansl et al., 2016). Global kelp forest communities are declining (Krumhansl et al., 2016); some kelp is directly negatively impacted by warming waters, others by the overspreading of sea urchins. Krumhansl and colleagues (2016) concluded that kelps forests are vulnerable to anthropogenic activities, including climate change, overfishing, and direct harvest.

The Effects of El Niño on Kelp

Environmental stress models (ESMs) and nutrient/productivity models (N/PMs) are two conceptual models that explain how local environmental conditions should influence communities (Connell, 1975; Menge & Sutherland, 1976, 1987; Fretwell, 1977, 1987; Oksanen et al.,1981; Menge & Olson, 1990; Menge, 2000; Menge & Branch, 2001). ESMs predict that food chain length decreases with increases in environmental stress. For example, the detrimental effects of El Niño on intertidal macroalgae also extend to subtidal environments. Giant kelp forests off the California coast often experience large scale mortality after severe El Niño events resulting in a loss of habitat and food for invertebrates, fish, and higher trophic animals (Dayton et al. 1992). However, N/PMs predict that the food chain would be lengthened with increased supply of nutrients (Menge et al. 1997; Menge, 2000; Oksanen et al. 1981).

Thus, the predicted consequence of an El Niño event differs depending on whether an ESM or N/PM mechanism is inferred. Increasing environmental stress can result in increasing productivity, like the severe reduction of kelp by warm nutrient depleted waters during the 1983-84 El Niño (Dayton et al. 1992). However, in the areas of strong and persistent upwelling, kelp was able to recover quickly or maintain its population due to an additional boost of nutrients (Dayton et al. 1992). Though El Niño tends to decrease kelp cover, recovery can happen quickly once El Niño ceases and upwelling resumes, as occurred after the 1983-84 El Niño (Dayton et al. 1992; Freidenburg et al. unpublished thesis chapter, 2002). Furthermore, experimentally added nutrients can increase kelp survival even under a stressful warm water conditions (Dayton, 1985; Korpinen et al., 2007; Russell & Connell, 2005).

Past studies show that El Niño has detrimental effects on the kelp communities. The 1997–1998 El Niño was the second highest recorded, and many macroalgal species declined from the Galápagos Islands (Vinueza et al., 2006) to the Oregon Coast (Freidenburg et al. unpublished thesis chapter, 2002; Menge et al., 2009).

Although El Niño events can have strong effects on the kelp communities, one study showed the abundance and growth of intertidal kelp recovered fully during La Niña years on the Oregon Coast due to elevated nutrients (Freidenburg et al. unpublished thesis chapter, 2002). Freidenburg studied this case from 1997 to 2000 after the 1997-98 El Niño; the rate of kelp recovery was positively correlated with the intensity of coastal upwelling. Indeed, kelps recovered more quickly at the Cape Blanco, where upwelling is stronger, than in central Oregon where it is weaker (Freidenburg et al. unpublished thesis chapter, 2002).

To test how the El Niño conditions in 2015-16 affected kelp populations and their subsequent recovery, I surveyed three species of intertidal kelp in central and southern Oregon from 2015–2018. I predicted that abundance and growth of kelp would be constrained by El Niño conditions in 2015-16 and would be recovered by summer 2018. I further predicted that the kelp recovery would be faster in southern Oregon than north Oregon due to higher upwelling. Thus, my research investigated how local and regional environmental processes modulated the effects of El Niño on kelp communities along the Oregon coast.

2. Methods

2.1 Study area

The Oregon Coast has natural spatial variation in physical and biological characteristics, which makes the coast an optimal area to study the responses of three common intertidal macroalgal species. Seven rocky intertidal sites on the Oregon coast were studied. These seven sites span 300 km off the coast in the Pacific Ocean (Figure 1) and they are characterized by an upwelling gradient. Cape Foulweather (CF), the northernmost study area, consists of three sites: Fogarty Creek (FC), Boiler Bay (BB), and Depoe Bay (DB). Cape Perpetua (CP), the central region, consists of two sites: Strawberry Hill (SH) and Yachats Beach (YB). And at the southernmost, the Cape Blanco (CB) consists of two sites: Cape Blanco North (CBN) and Rocky Point (RP). Cape Foulweather is exposed to weaker, intermittent upwelling compared to Cape Blanco with stronger and persistent upwelling and the coastal topography varies from site to site. Upwelling start earlier in the spring for southern Oregon (Freidenburg et al. unpublished thesis chapter, 2002). Three common intertidal macroalgal species were studied and are found at the similar degree of wave exposure at each site. All sites excluding DB had *Saccharina sessilis* and *Egregia menziesii*. *Postelsia palmaeformis* are only found in FC, DB, YB and CBN sites. They are commonly found on the headlands or outcrops at the lowest of low tide zones.

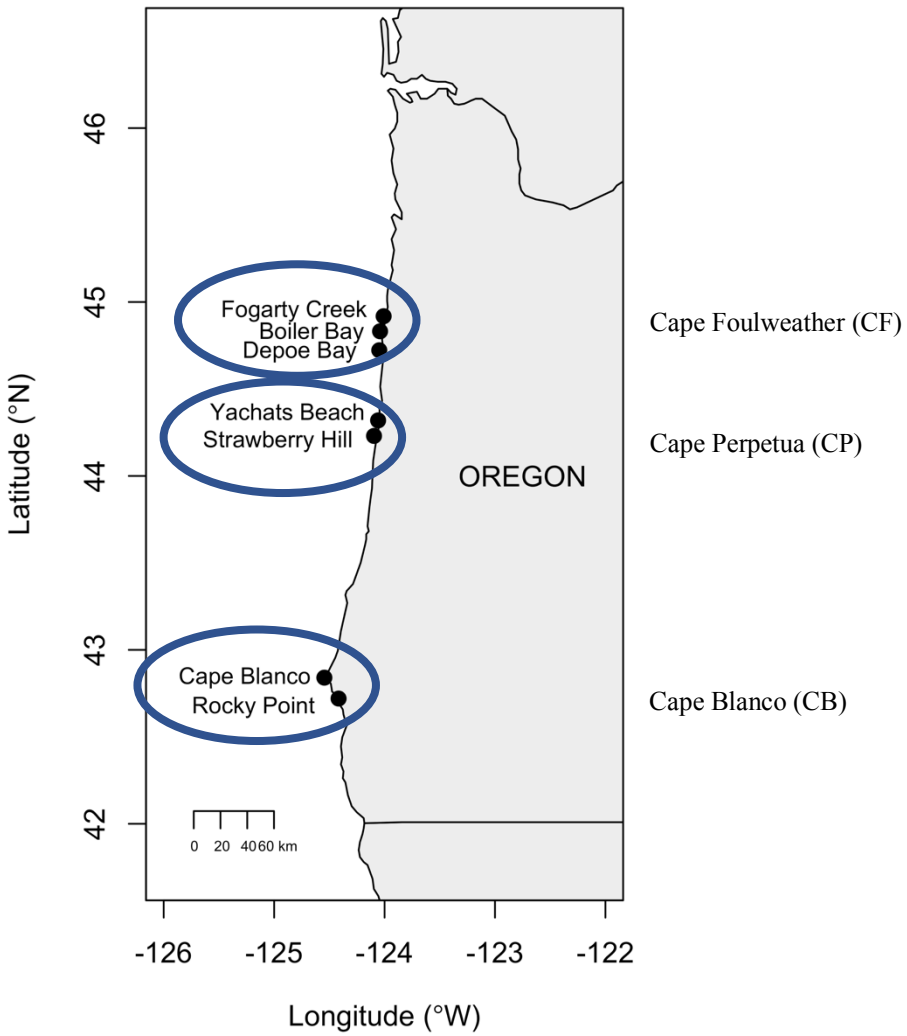

Figure 1. Map of study sites along the Oregon Coast. FC, BP and FC are on the north Oregon Coast. YB and SH are on the central Oregon Coast and CBN and RP are in the Cape Blanco, the southernmost region of the Oregon Coast.

2.2 Time Span

Researchers conducted a similar project from 1998 to 2000, after the 1997 El Niño (Friedenburg et al. unpublished thesis chapter, 2002). Their methods were repeated for this study in an effort to produce a comparison between two major El Niño events (1997-98 and 2015-16) and to better understand the strength of El Niño on spatiotemporal scales. This study was conducted from May, June and July from 2016 to 2018. At each study site, measurements were collected monthly during the lowest tides.

2.3 Overview of study organisms

Postelsia palmaeformis, Egregia menziesii and Saccharina sessilis are three common intertidal macroalgal species in the order Laminariales (Figure 2), commonly known as kelp. *P. palmaeformis* is an intertidal annual brown alga and is found on wave exposed area in patches. During the macroscopic sporophyte cycle, it resembles a small palm tree. The strong and flexible stipe allow it to stand in wave exposed areas. It settles on beds of *Mytilus*

californianus mussels, the competitive dominant space occupier in the region (Dayton, 1973). *P. palmaeformis* sporophytes grow during the spring and summer, and become reproductive from May to June (Blanchette, 1996). Fall and winter storms remove mature sporophytes, permitting space for new recruits (Blanchette, 1996; Dayton, 1973; Paine, 1979, 1988).

Figure 2. Three kelp species pictured; *S. sessilis* (top left), *E. Menziesii* (top right) and *P. Palmaeformis (Bottom)*

E. menziesii and *S. sessilis* are biannual plants. *S. sessilis,* called as Sea Cabbage, is a dark brown kelp found on rocks in the low to mid intertidal in both wave-exposed and wave-protected areas. This kelp has large blades growing from a large holdfast without a stipe. It occurs from the Aleutian Islands, Alaska to Monterey, California (Agardh, 1824). *E. menziesii menziesii,* known as Feather Boa kelp, is a brown kelp and are commonly found on lower intertidal rocks. The kelp has long rachis growing from a thick holdfast and is mostly reproductive during spring and summer (Freidenburg et al. unpublished thesis chapter, 2002). It is distributed from Alaska to Baja California in both protected to moderately wave-exposed areas (Abbott & Hollenberg, 1976).

2.4 Quantification of macroalgae communities

Populations demographics (algal abundance and size) of the three focal macroalgal species were investigated using algal grid surveys along the Oregon coast. *S. sessilis, E. menziesii* and *P. palmaeformis* were sampled monthly in May, June and July from 2016 to 2018 at low intertidal zone, to quantify their relative abundance and size. Five 5m permanent transects were established in 2016 for each species at each site where the target species appeared abundant. After the first year, the same permanent transects were surveyed with quadrats. The abundance and size was recorded within 0.5 m^2 quadrats placed contiguously on both sides of the transects, resulting in 20 quadrats total (Figure 3).

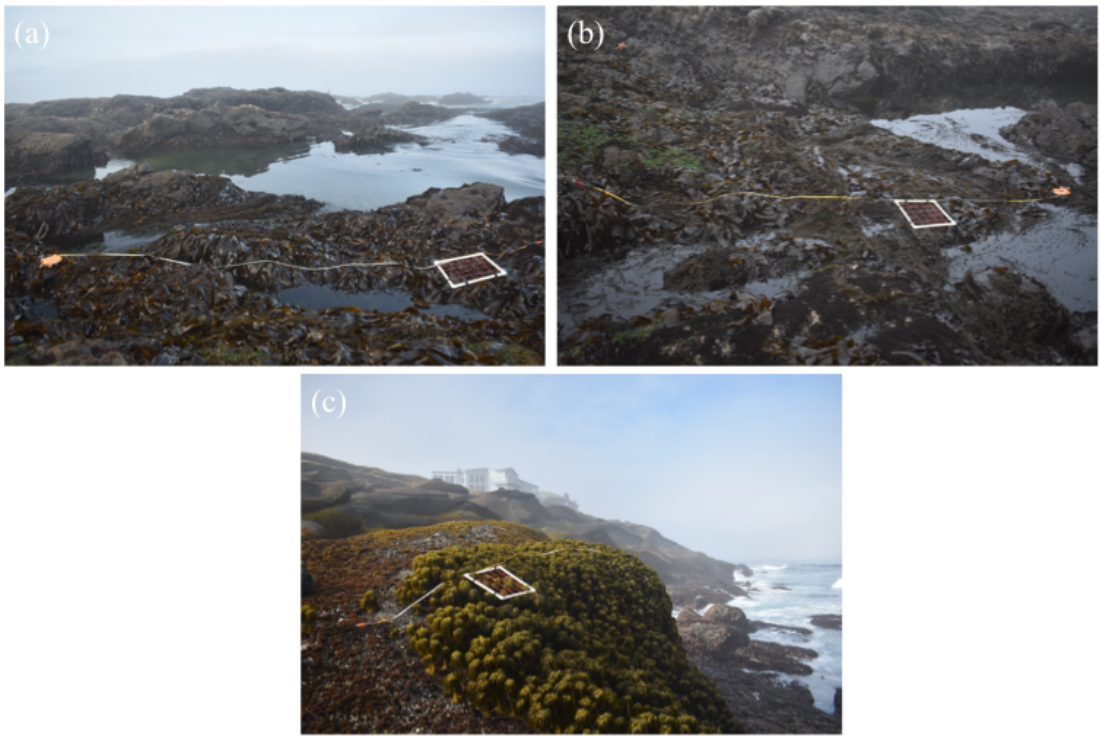

Figure 3. Algal Grid surveys of *S. sessilis* (a), *E. menziesii* (b) and *P. palmaeformis* (c) at lowest tides. The survey included the estimation of percent cover, density and length using quadrat.

The percent cover, density, and length were measured. Percent cover was the visual estimation of total algae cover in each quadrat. Indeed, quadrats were subdivided into 25 10X10 cm^2 squares and each square represents 4% of the total area enclosed by the frame. The density was the count of individual holdfasts in each quadrat; and length was measured in centimeters using the longest frond in each quadrat. The frond lengths were measured for *S. Sessilis and E. Menziesii,* and the stipe and frond length were measured for *P. palmaeformis.* Only the stipe length for *P. palmaeformis* was presented in this study. If a transect was designated for a particular species of macroalgae, then that particular species would only be measured and other species would be excluded. The competition between algae and other species were not included in the study.

2.5 Environmental parameters

Parameters that may have effects on the abundance and size of kelp communities were investigated, including Sea Surface Temperature (SST), Dissolved Inorganic Nitrogen (DIN), Chlorophyll (Chl-a), upwelling, wave action, Multivariate ENSO Index, the Pacific Decadal Oscillation and the North Pacific Gyre Oscillation.

2.5.1 At meso-scale

First, Sea Surface Temperature (SST), Chlorophyll, Dissolved Inorganic Nitrogen (DIN) were collected by my colleagues at the Partnership for Interdisciplinary Studies of Coastal Oceans (PISCO). SST was measured using the temperature loggers fixed on the rocks in the low tide zone. The loggers recorded data every 5 min at all sites (except DB) over the upwelling season from May to July. For my analysis, I averaged the data to acquire monthly means at each site. Some data were missing due to logging errors. Nutrients were measured in the form of Inorganic N, nitrate + nitrite and phytoplankton were measured in the form of chl *a*. Inorganic nitrogen is a primary limiting macronutrient in the marine ecosystems and phytoplankton are also consumers of inorganic nutrients. Water samples for the Chlorophyll-a and Dissolved Inorganic Nitrogen were collected monthly in triplicate at each site at low tide (Menge et al., 2015). Chlorophyll and DIN were measured in µg/L and µM, respectively and the values of the three samples were averaged to monthly means at each site (expect DB) in May, June and July from 2016 to 2018.

Wave action index is a measurement of the significant wave height in meters (SWVHT). The data for this study were acquired by the National Weather Service at NOAA (downloaded from their website). SWVHT is calculated as the average of the highest one third of all the wave heights during the 20-minute sampling period and is collected hourly every day per month and is located at 44.677 N 124.515 W, 20 NM West of Newport located between CF and CP. I averaged data from hourly to monthly from May to July in 2017 and June to July in 2018.

Upwelling Index was collected by the Pacific Fisheries Environmental Laboratory (PEFL), NOAA and were derived from synoptic (6-hourly) sea level pressure gridded fields by PFEL. The monthly upwelling index (downloaded from their website) was located at 42N 125W and was based on estimates of offshore Ekman transport driven by geostrophic wind stress. This point is representative of the Oregon coast upwelling and has no unit. The upwelling index was high during spring and summer (Figure 4).

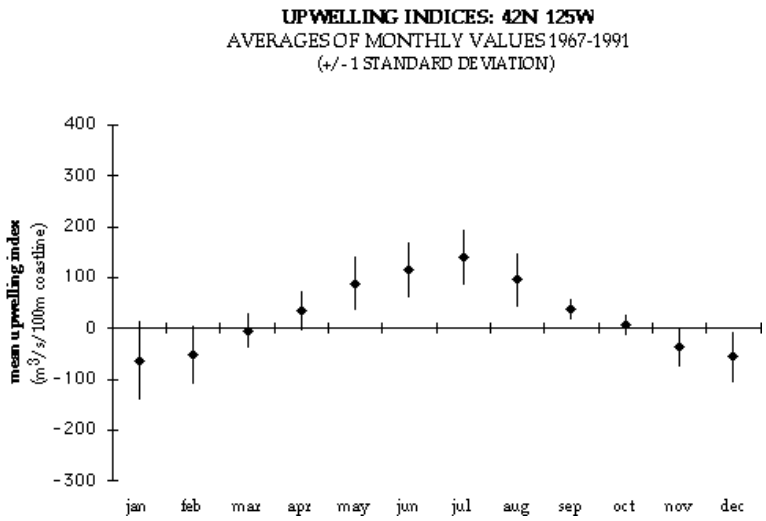

Figure 4. Average of monthly values of the upwelling index at 42N 125W from 1967 to 1991. (NOAA)

2.5.2 At macro-scale

To measure El Niño, I used the Multivariate ENSO Index (MEI), which is based on six variables: sea-evel pressure, zonal and meridional components of the surface wind, sea surface temperature, surface air temperature, and total cloudiness fraction of the sky. It is estimated by the Earth System Science Laboratory, NOAA. The MEI indicated El Niño (red and MEI positive) and La Niña (blue and MEI negative) (Figure 5). Since 1950, variations of the ENSO were recorded and we can see their evolutions on the figure. El Niño in 2015–2016 is one of the strongest events, albeit less stronger than the 1997–1998 and the 1982–1983 events.

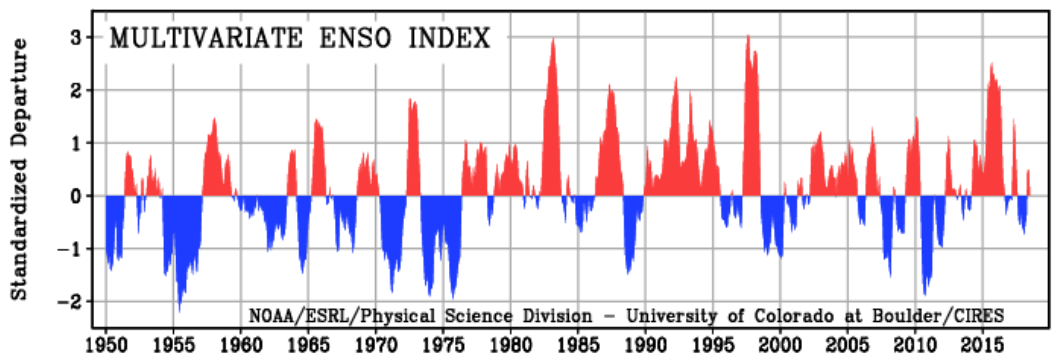

Figure 5. ENSO Time-series from 1950 to 2015

Pacific Decadal Oscillation (PDO) is measured by NOAA and it is often described as a pattern of Pacific Climate variability similar to ENSO, which also includes the warm and cool phases, as defined by ocean temperature anomalies in the Northeast and tropical Pacific Ocean. North Pacific Gyre Oscillation (NPGO) is measured by Dr. DiLorenzo with The Regional Ocean Modeling System (ROMS) (Di Lorenzo et al., 2008). The MEI, PDO and NPGO (downloaded from their website respectively) are linked and are large scales environmental factors. They are recorded monthly as one data point for the North Pacific Ocean. The MEI is

computed separately for each of twelve bimonthly seasons (Dec/Jan, Jan/Feb, Nov/Dec). I selected the number as the first month indicated (May for May/June, June for June/July and July for July/August).

2.5.3 Data frame

I compiled all data from May, June and July from 2016 to 2018 into one sheet (Table 1), ordered by Year, Month, Cape, Site, Species, transect label (5 for each species), quadrat label (20 for each transect), and three biological responses per quadrat: percent cover, density and length. Then I added columns for environmental factors. To match the biological sampling period, I replicated environmental factor data for each quadrat in all sites/capes and all months/years. Some data were missing due to no active sampling at the time.

Table 1. Visualization of data frame (these two separate tables are linked into one long row in the data sheet)

Year	Month	Cape	Site	Species	Transect	Quadrat	Percent cover	Density	Frond length	Stipe length
2016	July	CP	YB	*P.palmaeformis*	5	6	18	12	18	23
2017	May	CB	CBN	*S.sessilis*	1	1	50	3	42	
2017	June	CB	RP	*E.menziesii*	3	18	52	1	17	

Chla Mean	Chla SE	DIN Mean	DIN SE	Twater mean	Twater SE	MEI	NPGO	PDO	Upwelling	SWVHT
74.708	5.934	15.490	1.183	11.840	2.090	0.186	-0.487	1.250	134.789	
1.268	0.304	6.760	0.501	10.220	1.100	1.039	-0.507	0.880	98.500	1.500
4.161	0.039	6.571	0.800	10.280	1.400	0.461	-0.224	0.790	17.000	1.682

2.6 Data analysis

My statistical analyses included data from 2016–2018. A mixed effects model was used for each biological response (percent cover and length), testing for difference among sites and capes across years for each species. The percent cover for *S. sessilis* and *E. menziesii* had a binomial distribution (the percent cover was converted into ratio) and for *P. palmaeformis,* the distribution was gamma family. Length had a gamma distribution for all species. The factors 'Year', 'Month', 'Site' and 'Cape' were included as fixed factors because they were of direct interest in this study. 'Transect' and 'Quadrat' were included as a random factor because the transects and quadrats were chosen randomly and represented a sample from the larger kelp population at each site. The final model for each species was determined by removing terms from a full model based on the Akaike Information Criterion (AIC). 'Year' and 'Month' were treated as categorical variables because of their non-linear relationships over time. All mixed models were constructed using the 'lme4' package (Bates et al., 2015) and post-hoc comparisons were made using the 'multcomp' package (Hothorn et al., 2008) in RStudio version 1.1.453. For these tests, I used matched surveys in May, June and July. Furthermore, I used Pearson correlation and Principal Component analysis (PCA) using the 'factoextra' package (Kassambara & Mundt, 2017) to assess how each biological response (percent cover, density and length) for each of the three species varied with different environmental factors: Chlorophyll-a, Dissolved Inorganic Nitrogen, Sea surface temperature, Multivariate ENSO Index, Pacific Decadal Oscillation, North Pacific Gyre Oscillation, Upwelling, and Wave action and I decided to select only *S. sessilis* because it was the most abundant species at each site. To avoid model over-parameterization and complex model interpretations, a separate model was created for each species.

3. Results

3.1 Spatiotemporal responses of three common intertidal macroalgae

3.1.1 Saccharina sessilis

The recovery rate (the rate of change in percent cover over time) of *S. sessilis* for all sites was high in the first year after the El Niño (2016–2017) and then slowed down in the second year (2017–2018). CF had the fastest rate of recovery in 2017 (Figure 6a) and the percent cover was almost two times higher than CP and CB ($p<0.001$; Table 1B). The high percent cover in CF is primarily driven by the high percent cover in BB. CB had the lowest percent cover than the other two capes in 2016 and its percent cover was indistinguishable from CP by 2018 ($p<0.001$, Table 1B). Percent cover increased significantly for CP and CB from 2016 to 2018 ($p<0.001$, Table 1B).

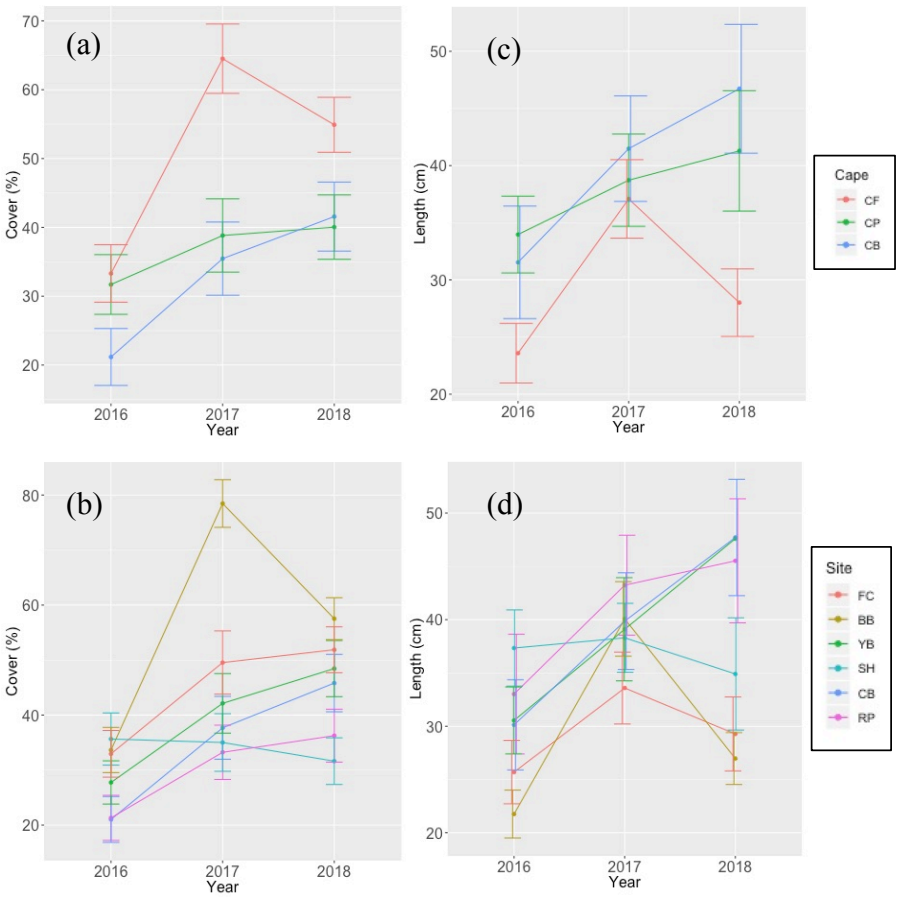

Figure 6. Percent cover of *S. sessilis* at three capes (a) and at six sites (b) and frond length of at three capes (c) and at six sites (d) five sites along the Oregon coast. Sites and Capes are arranged in latitudinal order with the northernmost site, BB and the southernmost site, CB, of each panel. In each case, values are averages of n=5 transects per site with bars representing standard error. Percent cover is the average proportion of area covered by *S. sessilis* and Length is the average distance from the holdfast to the end of the stipe.

Frond length was significantly higher at CB compared to CF in 2016 ($p<0.001$, Table 2B) and 2018 ($p<0.001$, Table 2B), with the average length approximately two times greater (Figure 3c); however, this was not significantly different from frond length CP in 2016 ($p = 0.5341$, Table2B) and 2018 ($p = 0.6780$, Table2B). *S. sessilis* in CB and CP had similar length but in CB had longer blade length that increased over the years from 2016 to 2018 ($p<0.001$, Table 2B) and significantly surpassed the length in CP in 2018 ($p <0.001$; Table 2B). This result showed the recovery in CB was faster than CP. All sites exhibited a general positive trend of having longer blade length over the years with an exception of YB, BB and FC (Figure 6d).

3.1.2 Egregia menziesii

Percent cover of *E. menziesii* did not differ significantly at the cape scale in 2016 (Figure 4a) but CP and CB had a significantly higher percent cover than CF in 2017 ($p = 0.0026$ and $p<0.001$ respectively, Table 1B). The percent cover in each cape decreased in 2018 with CB and having lower percent cover than CP ($p =0.0423$, Table 1B).

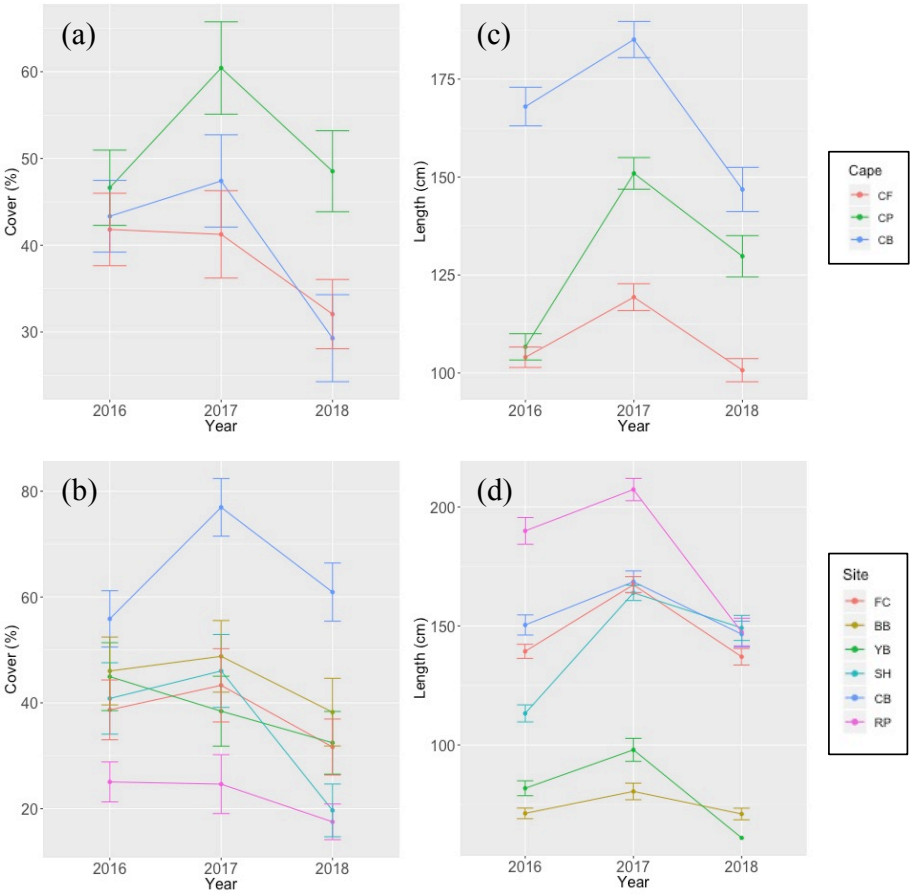

Figure 7. Percent cover of *E. menziesii* at 3 capes (a) and at six sites (b) and frond length of at 3 capes (c) and at six sites (d) five sites along the Oregon coast. Sites and Capes are arranged in latitudinal order with the northernmost site, BB and the southernmost site, CB, of each panel. In each case, values are averages of n=5 transects per site with bars representing standard error. Percent cover is the average proportion of area covered by *E. menziesii* and length is the average distance from the holdfast to the end of the stipe.

All capes exhibit the similar trends over the years with increases in percent cover in 2017 (Figure 7b) and decreases in 2018, but this trend was not statistically significant for the years 2016–2017 ($p = 0.7029$ for CB, $p = 0.2912$ for CF, $p = 0.2099$ for CP, Table 1B). SH had the highest percent cover of all sites ($p<0.001$; Table 1A). CP had higher average percent cover than CF in 2017, and CB in 2018 ($p<0.01$ and $p = 0,0423$, respectively, Table 1B) but not differ in 2017 ($p= 0.9999$, Table 1B).

We observed similar trends for length from 2016 to 2018, with increases in length in 2017 and decreases in 2018, in all capes ($p<0.001$ for CB, $p<0.01$ for CP and CF, Table 2B) (Figure 4c). *E. menziesii* at CB were significantly longer than at CF and CP for all years with RP having the longest individuals ($p<0.001$, Table 2B) (Figure 7d). The largest difference was shortly after the El Niño in 2016 ($p<0.001$, Table 2B).

3.1.3 Postelsia palmaeformis

Percent cover in CB exhibited a positive trend with a significantly higher cover in 2018 than 2016 ($p<0.001$, Table 1B) (Figure 5a). Percent cover did not differ between CB and CP in 2016 ($p = 0.9999$, Table 1B); however, by 2018 the cover in CB was almost 30% higher than CP ($p<0.001$, Table 1B). Percent cover in CF (both FC and DB, Figure 8b) decreased from 2016 to 2018 ($p<0.001$, Table 1B).

Length of *P. palmaeformis* in CB exhibited a positive trend over the years (Figure 8c) and had surpassed the other capes by 2018 ($p<0.001$, Table 2B). In 2016, *P. palmaeformis* in CB was almost 2.5 times longer than in CP ($p<0.001$ from CF and $p<0.01$ from CP, Table 2B). CB and CP exhibited a similar behavior in 2016 and 2017 but in 2018 they differ with length being four times longer in CB ($P<0.001$, Table 2B). Length of *P. palmaeformis* in CF, both FC and DB (Figure 5d), decreased over the years ($P<0.001$, Table 2B).

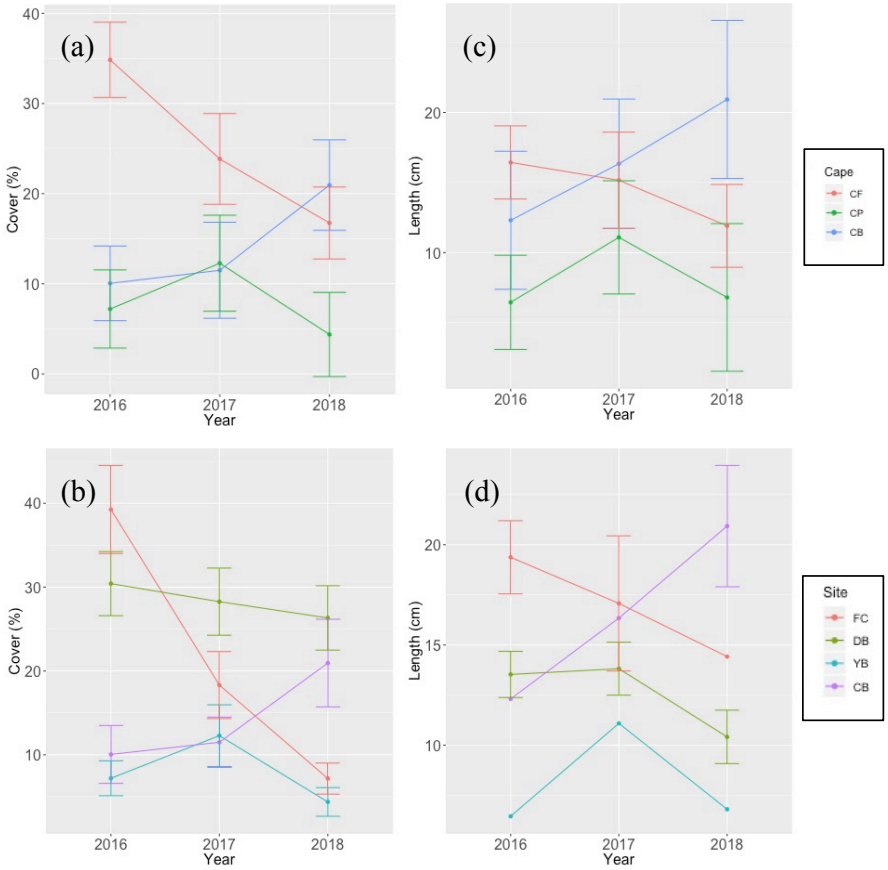

Figure 8. Percent cover of *P. Palmaeformis* at 3 capes (a) and at four sites (b) and stipe length of at 3 capes (c) and at four sites (d) along the Oregon coast. Sites and Capes are arranged in latitudinal order with the northernmost site, FC and the southernmost site, CB, of each panel. In each case, values are averages of n=5 transects per site with bars representing standard error. Percent cover is the average proportion of area covered by *P. Palmaeformis* and length is the average distance from the holdfast to the end of the stipe.

3.2 Seasonal variability

Inter-seasonal variability was not assessed as there were no data available for fall, winter, and spring; however, intra-seasonal variability can be assessed for the summer season (Figure 9). *S. sessilis, E. menziesii, and P. palmaeformis* in all sites showed a general increasing trend in percent cover over the months with the highest percent cover in July. *S. sessilis* percent cover increased over the years for all months from 2016 to 2018 in most of the sites. While *E. menziesii* and *P. palmaeformis* on the other hand, showed a more variable trend. *E. menziesii* had a upward-downward pattern with 2017 having the highest percent cover for all months and 2018 having the lowest percent cover. *P. palmaeformis* had no clear patterns. In FC, the percent cover of *P. palmaeformis* consistently decrease over the years for all months. In CB, the trend was reversed – the percent cover increased over the years for all months.

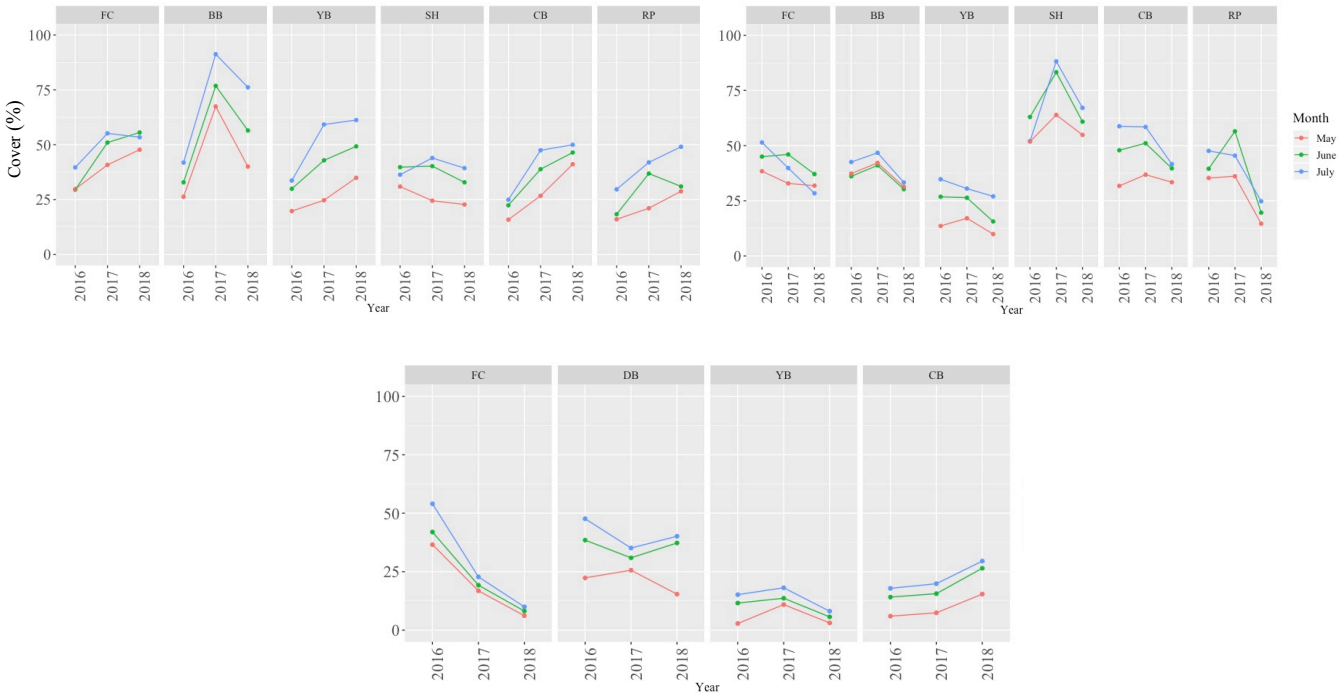

Figure 9. Monthly average percent cover in *S. sessilis* (top left), *E. menziesii* (top right) and *P. palmaeformis (bottom)* from 2016 to 2018.

3.3 Environmental factors

Environmental data were analyzed to reveal if any large-scale variation in environmental factors were associated with the observed pattern of intertidal algae abundance. El Niño conditions (high MEI) were moderately and slightly negatively correlated with length (correlation = -0.43, Table 3) and percent cover (correlation= -0.36, Table 3), respectively. Chlorophyll-a exhibited a similar pattern to *S. sessilis* length (Figure 11, Index I). SST was more persistent in 2015–2016 than 1996–1997 and the amplitude of the mean sea surface temperature increased considerably over years in the Oregon Coast. Sea surface temperatures were over 3 °C from the average of sea surface temperature in 1997 and 2016 (Figure 12, Index I). Meanwhile, the sea surface temperature was slightly negatively correlated with length (correlation = -0.16, Table 3). Nutrients and chlorophyll-a data showed a similar pattern to sea surface temperature. Nutrient and chlorophyll-a concentrations generally increased during the spring and summer due to upwelling (correlation=0.37 for DIN and 0.48 for chlorophyll-a). During the post-El Niño period, chlorophyll-a concentrations differed among the regions. The seasonal mean chlorophyll-a concentration (Figure 10) were found to be high during the spring and summer and lower during the autumn. The monthly mean chlorophyll-a concentration from 2013 to 2018 indicates high chlorophyll-a concentration during July in SH. SH had consistently higher chlorophyll-a concentration than any other sites.

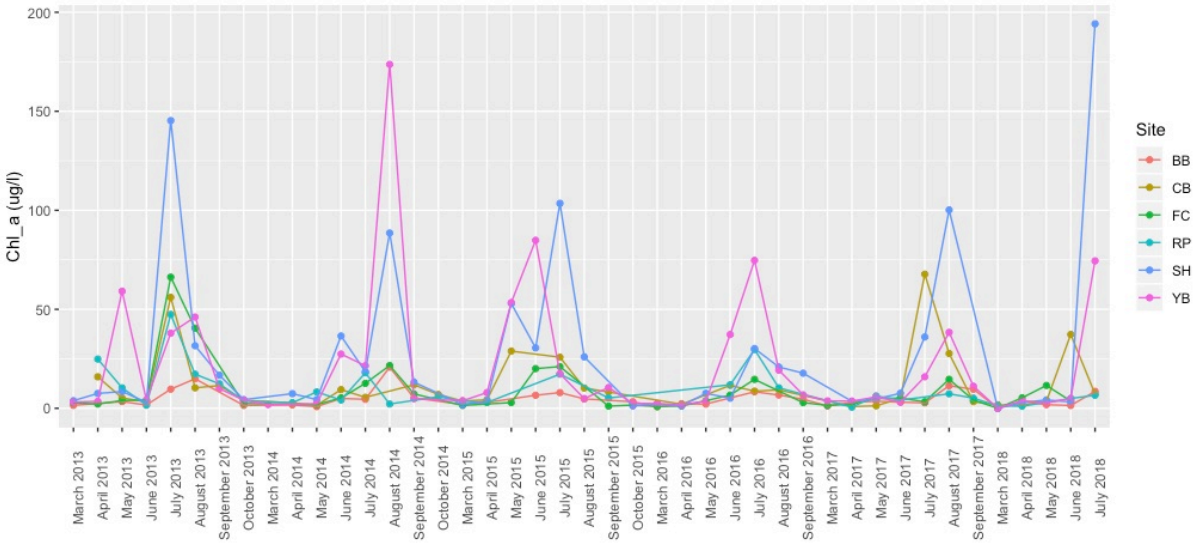

Figure 10. Variability of chlorophyll-a (chl-*a*) concentration during 2013–2018 covering the Oregon coast waters from BB to CB

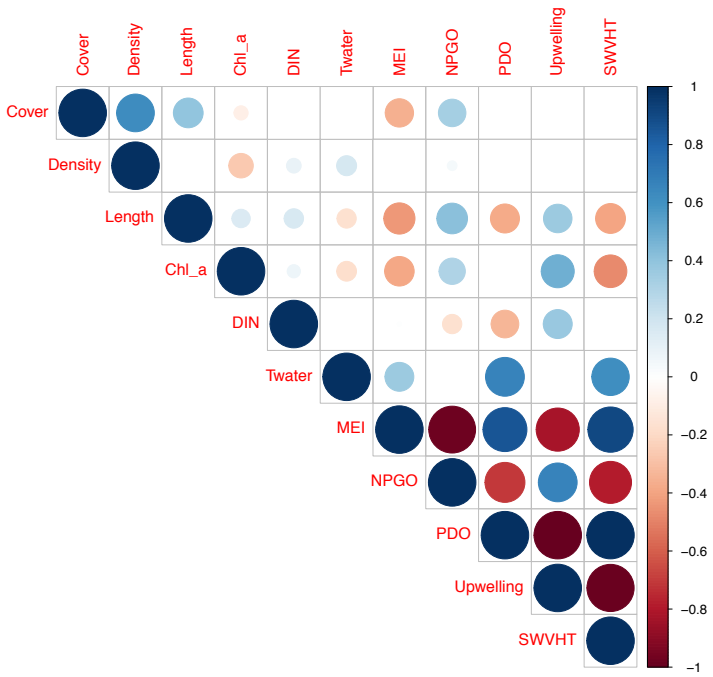

Figure 11. Analysis of correlation between environmental factors and variables responses for *S. sessilis.* The positive correlation is shown in blue, while the negative correlation is shown in red. The color and size represent the magnitude of correlation. The correlations with p-value> 0.01 are considered as insignificant and are left blank.

3.4 Local and regional spatial variability of distribution of *Saccharina sessilis*

To evaluate the spatial distribution of *S. sessilis,* I compared biological responses and environmental factors using PCA. The PCA variability explained 87.6% of total variance of the data. This analysis revealed (Figure 13) that cape and site had an effect on kelp performance. *S. sessilis* appeared the most abundant in BB and the longest in CB. The three capes were distinct by a spatial environmental factors. CP region seemed be correlated with nitrate concentration while SH indicated a high chlorophyll-a concentration.

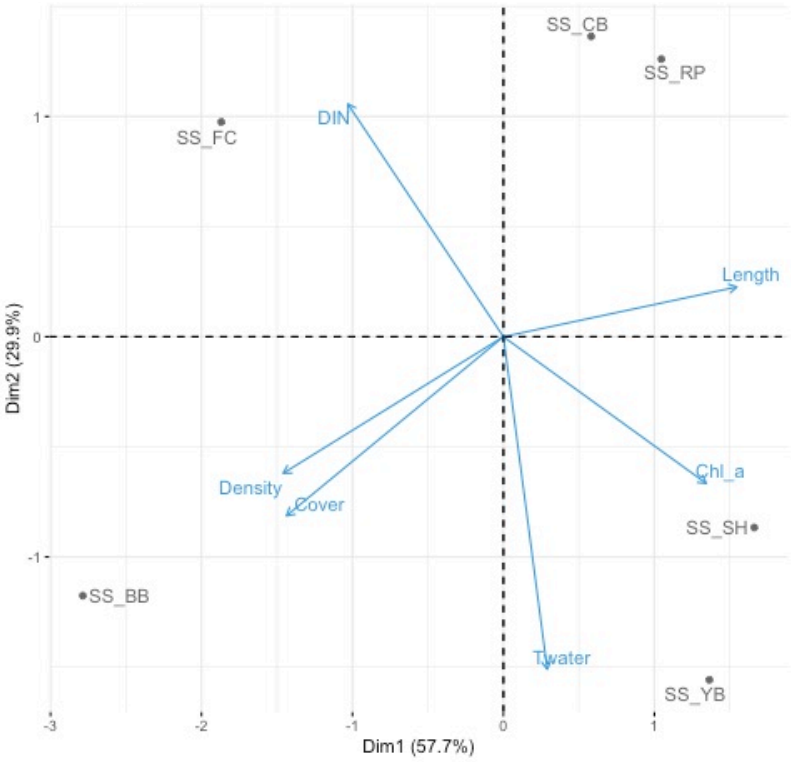

Figure 13. Principal components analysis of the spatial variability from *S. sessilis.*

3.5 Comparison with Freidenburg's papers

A comparison of my results with Freidenburg's thesis enabled me to observe the recovery of three common macroalgae species post El-Niño in 1997–1998 and in 2015–2016. Freidenburg studied the recovery of *S. sessilis* in percent cover for BB and SH (Figure 14); the recovery of *E. mensizeii* for BB, SH and CB*;* the recovery of *P. palmaeformis* for FC, DB, YB and CB for *P. palmaeformis* (Figure 15). The percent cover was much higher in 2018 than 2000 for *S. sessilis*. However, the percent cover was lower in 2018 than 1999 for *E. menziesii and P. palmaeformis.*

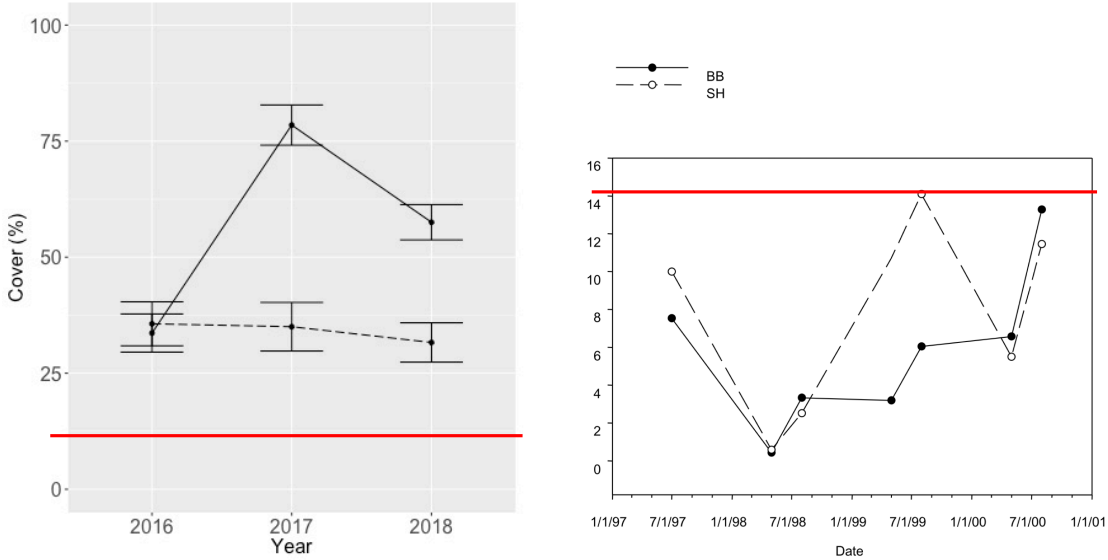

Figure 14. A post El Niño comparison of the intertidal macroalage recovery in percent cover for *S. sessilis* in 2016 to 2018 (on the left) and in 1997–2001 (on the right). Solid and dashed lines represent percent cover of *S. sessilis* in BB and SH, respectively. Red line represents the highest percent cover of *S. sessilis* between 1997 and 2000

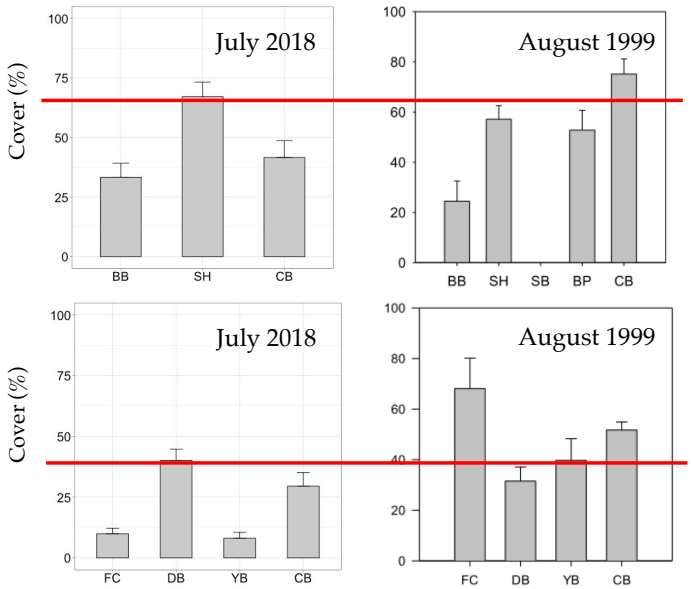

Figure 15. A post El Niño comparison on *E. menziesii and P. palmaeformis* recovery in percent cover in 2018 (on the left) and in 1999 (on the right). Red line represents the average percent cover of *E. menziesii and P. palmaeformis* in 1999.

4. Discussion

The results provided an insight into how local and regional environmental processes modulate the strength of El Niño and its effects on the recovery of kelp communities along the Oregon coast. There is a marked difference in recovery trajectories of intertidal macroalgae along the Oregon coast after the 2015-16 El Niño. Intertidal kelp abundance and size were reduced by a large scale El Niño event in 2015–2016. Intertidal algae demonstrated a general trend of increasing abundance over the years from 2016 to 2018, with a strong recovery rate in the first year.

BB had the highest percent cover of *S. sessilis* of all sites during 2016–2018 and had the largest increase in length from 2016 to 2017. Reasons for the high cover and long individuals remain unknown but the geographic features of BB may provide optimal growing conditions. The site has a narrow and sheltered chasm that was created by erosion. The chasm provides a protection for the kelp by breaking waves (Corcoran, 1965). Additionally, BB has a predominantly basalt rock formation and it may provide a solid foundation for holdfast attachment.

E. menziesii and P. palmaeformis experienced high mortality from 2016 to 2018. The percent cover of *P. palmaeformis* in CB increased over the years, while the cover in FC, DB, and YB decreased. The percent cover of *E. menziesii* was highest in SH. These responses could be explained by a combination of species identity and species' physical location within the sites. *E. menziesii* and *P. palmaeformis* are sensitive to wave exposure and are easily broken or dislodged under in high wave conditions (Blanchette et al., 2002; Blanchette, 1996; Paine, 1979). *P. palmaeformis* are normally found on the edge of rocks at the headlands or outcrops and are directly impacted by waves. Because CBN has lower wave action than FC, DB, and YB, *P. palmaeformis* were able to persist, thus resulting in a higher percent cover. *E. menziesii,* on the other hand, are found in exposed areas in all of the sites except for SH. In SH, they are situated behind a sea wall sheltered from the waves.

Growth of intertidal kelps is intimately linked to nutrients and sea surface temperature (Menge, 2000). Percent cover of *P. palmaeformis* and *S. sessilis* were much lower in CB in the first year following the El Niño. Because there were no surveys before the El Niño event, there is no baseline to compare the abundance pre- and post-El Niño to recognize whether the low abundance is an attribute of the region. However, the results show that kelp appeared to reach its stable abundance by 2017 as the cover was not significantly different between 2017 and 2018. CB has a lower percent cover of *S. sessilis* than the other two capes in 2016; however, the population recovered quickly over the years and its percent cover was indistinguishable from CP by 2018. The length was greater in CB for *S. sessilis* in 2018 (CP comes in a close second) and *P. Palmaeformis* over the three years. The regional responses of *S. sessilis* and *P. palmaeformis* can be explained by differences in coastal topography and oceanographic processes.

CB and CP receive nutrient inputs from intermittent upwelling episodes in the spring/summer. Because CP has a wide continental shelf, it creates retentive currents that allow nutrient-laden waters to stay in the shelf for an extended period of time. Nutrients stimulate phytoplankton blooms that block the light from penetrating the water column, thus shading benthic macroalgae (Kavanaugh & Menge, 2005). So, a combination of ample nutrients and shading may contribute to the length of *S. sessilis* being second to CB. However, coastal upwelling in the south region occurs more frequently than the central and north regions. Therefore, intertidal kelps in the south will have more access to nutrients; this may explain why they recover quickly in CB.

El Niño will depress thermocline and raise the sea surface temperature along the Oregon coast. Upwelling may bring warm nutrient-depleted water in addition to cold nutrient-rich

water. Because upwelling is more frequent in the southern region, kelp in CB could be more exposed to warmer waters and had reduced access to nutrients. This change in environmental conditions could cause kelp to become stressed, thus making them susceptible to winter storms (Dayton et al., 1992). Because the El Niño event is also accompanied by strong swells and high sea level, which will have strong consequences on intertidal kelps (Vinueza et al., 2006). When normal conditions returned after the 2015-16 El Niño, the sea surface temperature appeared colder, indicating the elevation of thermocline (the warm layer is decreasing) and upwelling of cold nutrient-rich waters, which in turn aided the recovery of macroalgal communities in the south.

Percent cover of *S. sessilis* after the 2015-16 El Niño were higher than the cover after the 1997-98 El Niño (Freidenburg et al. unpublished thesis chapter, 2002). The sea surface temperature was one degree higher the year preceding 1997 (the second-strongest El Niño in the recorded history) than the year preceding 2015 (the third-strongest El Niño) in the California Current System (Jacox et al., 2016). Because the 2015-16 El Niño was less strong than the 1997-98 El Niño, it had a weaker effect on the intertidal kelps. In the contrast, *E. menziesii* and *P. palmaeformis* abundances were much lower after the 2015-16 El Niño. Many individuals were either broken or dislodged by strong waves. Freidenburg indicated in her study that there were no strong waves between 1997 to 2000. The cause of the strong waves in the recent years needs to be explored.

Upwelling data from NOAA show the pattern of upwelled waters were generally constant over the period of my study (from May to July, from 2016 to 2018) on the Oregon coast. The result is consistent with those of Wang et al. (2015), indicating upwelling is not intensifying over time. However, sea surface temperature shows that the temperature is becoming warmer over time. The warming will result in more pronounced stratification in the ocean and depress the thermocline (Roemmich & McGowan, 2014; Wang et al., 2015). The thermocline depression will decouple the upwelling-nutrient system as upwelling will bring warmer, nutrient-depleted waters, which could have severe implications for the recovery of macroalgal community after an El Niño event in the future. CB is shown to provide a refuge for the kelp due the strong gradient of upwelling but the strength of large-scale temporal changes may trump regional differences, thus rendering the localized refuge inhospitable.

Climate change may not alter the frequency and intensity of coastal upwelling in the California Current System but it may alter the chemistry of upwelling. However, climate change may contribute to the intensification of El Niño on a larger scale with persistent and violent storms (Jacox et al., 2016). In the tropical Pacific, the total duration of the 2015–2016 El Niño was longer than the 1997-98 El Niño (Hu & Fedorov, 2017). Storms enhanced by El Niño and climate change in addition to ocean stratification and warm, nutrient-depleted waters produced by upwelling could cause severe and long-lasting consequences on the ecologically and economically important kelp communities. Despite our understanding on the impact of the climate change, the consequences on El Niño is still unclear. Thus, the impact of macroalgal communities is still uncertain.

The links between climate change and oceanographic patterns such as El Niño-Southern Oscillation and coastal upwelling remain unclear. This research shows that local and regional processes do modulate the strength of El Niño on the intertidal kelp communities. However, persistent large-scale climatic processes (i.e., warming) could shift the relationship between upwelling and kelp communities from beneficial to harmful.

5. Conclusion

This research centered around two questions: (1) what do recovery trajectories of intertidal macroalgae look like post-El Niño and how do they differ along the Oregon coast?, and (2) what are the major physical factors that modulate the relative strength of El Niño on intertidal macroalgae? I hypothesized that abundances of intertidal macroalgae will decrease after an El Niño event and recover fully within two years. Additionally, macroalgae in the southern Oregon will recover more quickly than macroalgae in the central and northern Oregon due to more persistent upwelling in the south. The results showed that local and regional environmental processes do modulate the strength of El Niño and its effects on the recovery of kelp communities along the Oregon coast. Intertidal kelp abundance and size were reduced by the 2015-16 El Niño event (more so in the southern Oregon) and they were recovered two years after the event with a faster recovery rate in the southern Oregon. The results hint at the possibility of upwelling being a double-edged sword in the face of persistent large-scale climatic processes (i.e., warming), shifting the beneficial relationship between upwelling and kelp communities to a harmful one. In order to better understand and anticipate future climate change ramifications on the intertidal kelp communities, a deeper analysis of kelp physiology is necessary to explain how kelp differ in their responses to varying environmental factors. In addition, the study should be conducted on a larger spatial and temporal scales to quantify links between climate drivers such as El Niño and biological communities.

References

Abbott, I. A., and Hollenberg G. J. (1976) Marine algae of California. *Stanford University Press*, Stanford, CA.

Agardh, C.A. (1824) *Systema algarum. Lundae, Literis Berlingianis*. doi:10.5962/bhl.title.1829

Bakun, A., Black, B. A., Bograd, S. J., Miller, A. J., Rykaczewski, R. R., & Sydeman, W. J. (2015). Anticipated Effects of Climate Change on Coastal Upwelling Ecosystems. *Curr. Clim. Change Rep,* 1, 85–93. doi: 10.1007/s40641-015-0008-4

Barber, R. T. (2008). Upwelling Ecosystems. *Encyclopedia of Ocean Sciences: Second Edition*, 225–232. doi: 10.1016/B978-012374473-9.00295-2

Bates, D., Maechler, M., Bolker, B., Walker, S. (2015). Fitting Linear Mixed-Effects Models Using lme4. *Journal of Statistical Software*, 67(1), 1–48. doi: 10.18637/jss.v067.i01

Blanchette, C. A. (1996). Seasonal patterns of disturbance influence recruitment of the sea palm, *P. palmaeformis*. *Journal of Experimental Marine Biology and Ecology*, *197*(1), 1–14. doi: 10.1016/0022-0981(95)00141-7

Blanchette, C. A., Miner, B. G., & Gaines, S. D. (2002). Geographic variability in form, size and survival of *E. menziesii* around Point Conception, California. *Marine Ecology Progress Series*, *239*, 69–82. doi: 10.3354/meps239069

Byrnes, J. E., Reed, D. C., Cardinale, B. J., Cavanaugh, K. C., Holbrook, S. J., & Schmitt, R. J. (2011). Climate-driven increases in storm frequency simplify kelp forest food webs. *Global Change Biology*, *17*(8), 2513–2524. doi: 10.1111/j.1365-2486.2011.02409.x

Connell, J.H. (1975) Some mechanisms producing structure in natural communities: A model and evidence from field experiments. *Ecology and evolution of communities*. Belknap Press, Cambridge, Massachusetts, 460–490

Corcoran, R. E. (1965) Geology of Lake Owyhee State Park and vicinity, Malheur County, Oregon. *The Ore Bin,* 27, 81–100.

Dayton, P. K. (1973). Dispersion, Dispersal, and Persistence of the Annual Intertidal Alga, *P. palmaeformis* Ruprecht. *Ecological Society of America* Stable, *54*(2), 433–438. doi: 10.2307/1934353

Dayton, P. K. (1985). Ecology of Kelp Communities. *Annual Review of Ecology and Systematics*, 16, 215–245. doi:10.1146/annurev.es.16.110185.001243

Dayton, P. K., Tegner, M. J., Parnell, P. E. & Edwards, P. B. (1992). Temporal and Spatial Patterns of Disturbance and Recovery in a Kelp Forest Community. *Ecological Monographs*, *62*(3), 421–445. doi: 10.2307/2937118

Di Lorenzo, E., Schneider, N., Cobb, K. M., Franks, P. J. S., Chhak, K., Miller, A. J., McWilliams, J.C., Bograd, S.J., Arango, H., Curchitser, E., Powell, T.M., Riviere, P. (2008). North Pacific Gyre Oscillation links ocean climate and ecosystem change. *Geophysical Research Letters*, *35*(8), 2–7. doi: 10.1029/2007GL032838

Falkenberg, L.J, Russel, D.B. & Connell S.D. (2012) Stability of Strong Species Interactions Resist the Synergistic Effects of Local and Global Pollution in Kelp Forests. *Plos one,* 7(3). doi: 10.1371/journal.pone.0033841

Freidenburg, T., Allison, G., Halpin, P., & Menge, B. (n.d.). Chapter 4: Effects of spatial and temporal variability in coastal upwelling on intertidal algae.

Fretwell, S.D., (1977) The Regulation of Plant Communities by the Food Chains Exploiting Them. *Perspectives in Biology and* Medicine, 20(2), 169-185. doi: 10.1353/pbm.1977.0087

Fretwell, S.D., (1987) Food Chain Dynamics: The Central Theory of Ecology?. *Oikos,* 50(3), 291–301. doi: 10.2307/3565489

Hothorn, T., Bretz, F. & Westfall, P. (2008), Simultaneous Inference in General Parametric Models. *Biometrical Journal*, 50(3), 346–363.doi: 10.1002/bimj.200810425

Hu, S. & Fedorov, A. V. (2017). The extreme El Niño of 2015–2016 and the end of global warming hiatus. *Geophysical Research Letters*, *44*(8), 3816–3824. doi:10.1002/2017GL072908

Jacox, M. G., Hazen, E. L., Zaba, K. D., Rudnick, D. L., Edwards, C. A., Moore, A. M. & Bograd, S. J. (2016). Impacts of the 2015–2016 El Niño on the California Current System: Early assessment and comparison to past events. *Geophysical Research Letters*,*43*(13), 7072–7080. doi: 10.1002/2016GL069716

Kassambara, A. & Mundt, F., (2017) Package 'factoextra'. *Extract and Visualize the Results of Multivariate Data Analyses*. https://CRAN.R-project.org/package=factoextra

Kavanaugh, M. T. & Menge, B. A. (2005). Phytoplankton Shading of Marine Benthic Macrophytes: Implications for Intertidal Community Structure. Oregon State University. 74–77. URL http://files/612/Kavanaugh Thesis.pdf

Korpinen, S., Jormalainen, V. & Honkanen, T. (2007). Effects of nutrients, herbivory, and depth on the macroalgal community in the rocky sublittoral. *Ecology*, *88*(4), 839–852. doi: 10.1890/05-0144

Krumhansl, K. A., Okamoto, D. K., Rassweiler, A., Novak, M., Bolton, J. J., Cavanaugh, K. C., Connell, S.D., Johnson, C.R., Konar, B., Ling, S.D., Micheli, F., Norderhaug, K.M., Pérez-Matus, A., Sousa-Pinto, I., Reed, D.R., Salomo,. AK, Shears, NT, Wernberg, T., Anderson, R.J., Barrett, N.S., Buschmann, A.H., Carr, MH, Caselle, J.E., Derrien-Courtel, S., Edgar, G.J., Edwards, M., Estes, J.A., Goodwin, C., Kenner, M.C., Kushner, D.J., Moy, F.E., Nunn, J., Steneck, R.S., Vásquez, J., Watson, J., Witman, J.D. & Jarrett, Byrnes, J.E.K. (2016). Global patterns of kelp forest change over the past half-century. *Proceedings of the National Academy of Sciences*, *113*(48), 13785–13790. doi: 10.1073/pnas.1606102113

McHugh, D.J (2003) A guide to the seaweed industry. *FAO Fisheries Technical Paper*. 441, 105.

Menge, B. A. (2000). Top-down and bottom-up community regulation in marine rocky intertidal habitats. *Journal of Experimental Marine Biology and Ecology*, *250*(1–2), 257–289. doi: 10.1016/S0022-0981(00)00200-8

Menge, B.A., Branch G.M., (2001) Rocky intertidal communities. *Marine community ecology*, 221–25.

Menge, B. A., Chan, F., Nielsen, K. J., Lorenzo, E. Di & Lubchenco, J. (2009). Climatic variation alters supply-side ecology: impact of climate patterns on phytoplankton and mussel recruitment. *Ecological Monographs*, *79*(3), 379–395. doi: 10.1890/08–2086.1

Menge, B.A., Daley, B. & Wheeler, P.A. (1996) Control of Interaction Strength in Marine Benthic Communities. Springer, Boston, MA. doi: 10.1007/978-1-4615-7007-3_26

Menge, B. A., Gouhier, T. C., Hacker, S. D., Chan, F., & Nielsen, K. J. (2015). Are meta-ecosystems organized hierarchically? A model and test in rocky intertidal habitats . *Ecological Monographs*, *85*(2), 213–233. doi: 10.1890/14–0113.1

Menge, B.A. & Olson, A.M. (1990) Role of scale and environmental factors in regulation of community structure. *Trends Ecol Evol,* 5(2), 52–57. doi: 10.1016/0169-5347(90)90048-I

Menge, B.A. & Sutherland, J.P. (1987) Community Regulation: Variation in Disturbance, Competition, and Predation in Relation to Environmental Stress and Recruitment. *The American Naturalist,* 130, 730–757. URL http://www.jstor.org/stable/2461716

Menge, B.A. & Sutherland, J.P. (1976) Species Diversity Gradients: Synthesis of the Roles of Predation, Competition, and Temporal Heterogeneity. *The American Naturalist*,110, 351–369. doi: 10.1086/283073

Oksanen, L., Fretwell, S.D., Arruda, J. & Niemela, P. (1981) Exploitation Ecosystems in Gradients of Primary Productivity. *The American Naturalist,* 118(2), 240–261. doi: 10.1086/283817

Paine, R. T. (1979). Disaster, Catastrophe, and Local Persistence of the Sea Palm *P. palmaeformis*. *Advancement Of Science*, *205*(4407), 685–687. doi: 10.1126/science.205.4407.685

Paine, R. T. (1988). Habitat Suitability and Local Population Persistence of the Sea Palm *P. palmaeformis*. *Ecology*, *69*(6), 1787–1794. doi: 10.2307/1941157

Roemmich, D. & McGowan, J. (2014). American Association for the Advancement of Science, *217*(4565), 1161–1163. doi: 10.1038/020493a0

Russell, B. D. & Connell, S. D. (2005). A novel interaction between nutrients and grazers alters relative dominance of marine habitats. *Marine Ecology Progress Series*, *289*, 5–11. doi: 10.3354/meps289005

Sydeman, W. J., Schoeman, D. S., Rykaczewski, R. R., Thompson, S. A., Black, B. A., & Bograd, S. J. (2014). Climate change and wind intensification in coastal upwelling ecosystems. *Science*, *345*(6192), 77–81.doi: 10.1126/science.1251635

Vinueza, L. R., Branch, G. M., Branch, M. L., & Bustamante, R. H. (2006). Top-down Herbivory and Bottom-up El Niño Effects on Galápagos Rocky-Shore Communities. *Ecological Monographs*, *76*(1), 111–131. doi: 10.1890/04-1957

Wang, D., Gouhier, T. C., Menge, B. A., & Ganguly, A. R. (2015). Intensification and spatial homogenization of coastal upwelling under climate change. *Nature*, *518*(7539), 390 –394. doi: 10.1038/nature14235

Wernberg, T., Thomsen, M. S., Tuya, F., Kendrick, G. A., Peter, A., & Toohey, B. D. (2010). Decreasing resilience of kelp beds along a latitudinal temperature gradient: potential implications for a warmer future. *Ecology Letters*, *13*, 685–694. doi: 10.1111/j.1461-0248.2010.01466.x

Wilmers, C. C., Estes, J. A., Edwards, M., Laidre, K. L., & Konar, B. (2012). Do trophic cascades affect the storage and flux of atmospheric carbon? An analysis of sea otters and kelp forests. *Frontiers in Ecology and the Environment*, *10*(8), 409–415. doi: 10.1890/110176

Xiu, P., Chai, F., Curchitser, E. N. & Castruccio, F. S. (2018). Future changes in coastal upwelling ecosystems with global warming: The case of the California Current System. *Scientific Reports*, *8*(1), 1–9. doi: 10.1038/s41598-018-21247-7

Webography

Earth System Research Laboratory, NOAA – National Oceanic and Atmospheric Administration URL https://www.esrl.noaa.gov/psd/enso/mei/ (accessed 13.6.18)

National centers for environmental information, NOAA – National Oceanic and Atmospheric Administration URL https://www.ncdc.noaa.gov/teleconnections/pdo/ (accessed 8.6.18)

National Weather Service, Environmental Modeling Center, NOAA – National Oceanic and Atmospheric Administration URL http://polar.ncep.noaa.gov/waves/viewer.shtml?-multi_1-US_eastcoast- / (accessed 10.6.18

Appendix I

Fig. 12 Differences of average of sea surface temperature (°C) from 1993 to 2018 in SH. The positive and negative difference is indicated in blue and orange respectively.

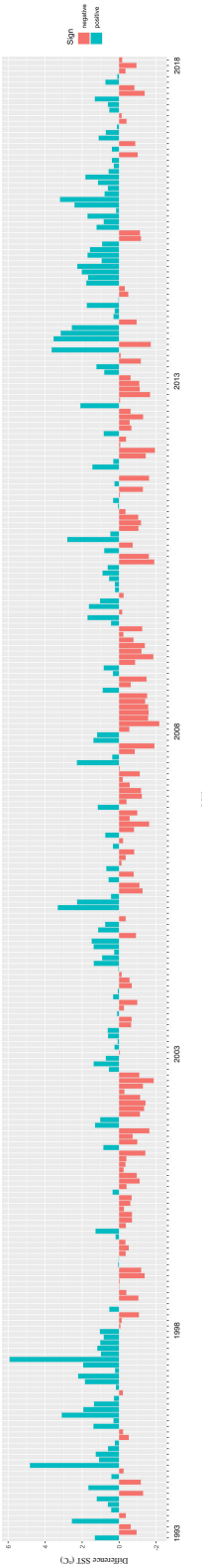

Appendix II

Average of upwelling index from 1990 to 2018 in the Oregon coas

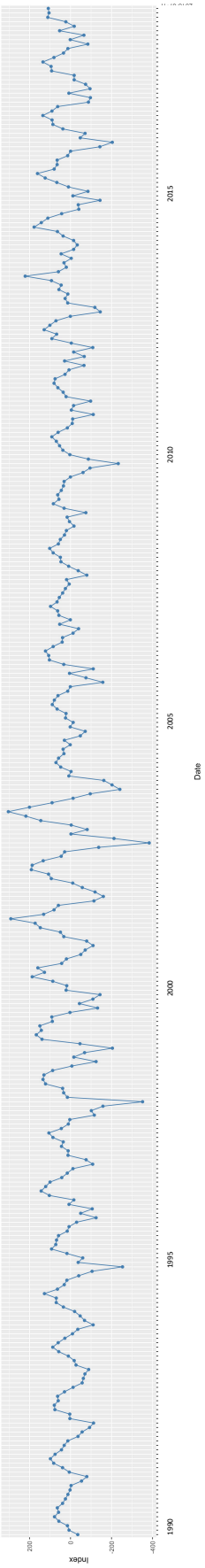

Appendix III

Table 1A. Effect of year, cape and site on the percent cover of the intertidal algae for the best-performing models. Results are from mixed effects models (LMER) with only fixed effects presented.

Species	Parameter	Estimate	Std. Error	z-value	p-value
Saccharina Sessilis	Intercept	-1.5281	0.22163	-8.811	P<0.001
	Year2017	1.65835	0.25565	6.487	P<0.001
	Year2018	2.21503	0.25125	8.816	P<0.001
	Month June	-0.57873	0.07705	-7.511	P<0.001
	Month May	-1.45218	0.08647	-16.794	P<0.001
	CapeCF	1.24514	0.26216	4.749	P<0.001
	CapeCP	1.36556	0.25994	5.253	P<0.001
	SiteFC	0.25297	0.19768	1.280	0.200647
	SiteYB	-0.82492	0.22661	-3.640	P<0.001
	SiteRP	0.33523	0.29153	1.150	0.250197
	Year2017:CapeCF	1.26301	0.33004	3.827	P<0.001
	Year2018:CapeCF	-0.68921	0.31349	-2.199	0.027912
	Year2017:CapeCP	-1.55880	0.32781	-4.755	P<0.001
	Year2018:CapeCP	-2.39848	0.32253	-7.439	P<0.001
	Year2017:SiteFC	-2.09968	0.27887	-7.529	P<0.001
	Year2018:SiteFC	-0.33599	0.26550	-1.266	0.205688
	Year2017:SiteYB	1.10327	0.30127	3.662	P<0.001
	Year2018:SiteYB	2.13752	0.29574	7.228	P<0.001
	Year2017:SiteRP	-0.57021	0.34822	-1.637	0.101533
	Year2018:SiteRP	-1.08456	0.35117	-3.088	P<0.001
Egregia menziesii	(Intercept)	-0.41423	0.15298	2.296	P<0.01
	Year2017	0.39287	0.17114	2.262	0.02170
	Year2018	-1.19806	0.21494	-5.574	P<0.001
	MonthJune	-0.16158	0.07803	-2.071	0.03838
	MonthMay	-0.64871	0.08091	-8.017	P<0.001
	CapeCF	-0.15666	0.17707	-0.885	0.37631
	CapeCP	-0.76754	0.25895	-2.964	0.00304
	SiteCB	0.34864	0.17442	1.999	0.04562
	SiteFC	0.49321	0.17387	2.837	P<0.01
	SiteSH	1.49530	0.25892	5.775	P<0.001
	Year2017:CapeCF	-0.16067	0.24559	-0.654	0.51297
	Year2018:CapeCF	0.54910	0.29040	1.891	0.05865
	Year2017:CapeCP	-0.72915	0.37410	-1.949	0.05129
	Year2018:CapeCP	0.60217	0.41109	1.465	0.14297
	Year2017:SiteCB	-0.35771	0.24192	-1.479	0.13924
	Year2018:SiteCB	0.69276	0.27829	2.489	0.01280
	Year2017:SiteFC	-1.07330	0.25514	-4.207	P<0.001
	Year2018:SiteFC	-0.08035	0.26464	-0.304	0.76142
	Year2017:SiteSH	1.65498	0.38574	4.290	P<0.001
	Year2018:SiteSH	1.04234	0.39003	2.672	P<0.01
Postelsia palmaeformis	Intercept	1.193735	0.047253	25.263	P<0.001
	Year2017	0.017973	0.014660	1.226	0.2202
	Year2018	0.109459	0.015301	7.154	P<0.001
	MonthJune	-0.041563	0.007951	-5.228	P<0.001
	MonthMay	-0.114803	0.007774	-14.767	P<0.001
	CapeCF	0.262666	0.013705	19.166	P<0.001
	Year2017:CapeCF	-0.167598	0.019166	-8.744	P<0.001
	Year2018:CapeCF	-0.308423	0.019380	-15.915	P<0.001
	Year2017:CapeCP	0.023551	0.020591	1.144	0.2527
	Year2018:CapeCP	-0.145456	0.020679	-7.034	P<0.001

Appendix IV

Table 1B. Pairwise comparison in percent cover post-hoc results from experimental analysis using Tukey for each species.

Species		Estimate	SE	Z ratio	p.value
Saccharina Sessilis	2016,CB - 2017,CB	-1.373245803	0.1742156	-7.882	P<0.001
	2016,CB - 2018,CB	-1.672753331	0.1757368	-9.519	P<0.001
	2016,CB - 2016,CF	-1.204008354	0.1761878	-6.834	P<0.001
	2016,CB - 2016,CP	-0.785493439	0.1846236	-4.255	P<0.005
	2017,CB -2018,CB	-0.299507528	0.1365345	-2.194	0.4097
	2017,CB - 2017,CF	-1.702280513	0.13708992	-12.417	P<0.001
	2017,CB - 2017,CP	-0.063432739	0.1376244	-0.461	0.9999
	2018,CB - 2018,CP	0.001947572	0.1361933	0.014	P<0.001
	2016,CF - 2017,CF	-1.871517961	0.1397247	-13.394	P<0.001
	2016,CF - 2018,CF	1.357821961	0.1333745	-10.181	P<0.001
	2016,CF - 2016,CP	0.418514915	0.1503507	2.784	0.1201
	2017,CF - 2018,CF	0.513696000	0.1319572	3.893	P<0.001
	2017,CF - 2017,CP	1.6388847773	0.1396693	11.734	P<0.001
	2018,CF - 2018,CP	-0.891024557	0.1300580	6.851	P<0.001
	2016,CP - 2017,CP	-0.651185103	0.1507951	-4.318	P<0.01
	2016,CP - 2018,CP	-0.885312320	0.1478050	-5.990	P<0.001
	2017,CP - 2018,CP	-0.234127216	0.1372601	-1.706	0.7433
Egregia menziesii	2016,CB - 2017,CB	-0.21401422	0.1209850	-1.769	0.7029
	2016,CB - 2018,CB	0.85167991	0.1391583	6.120	P<0.001
	2016,CB - 2016,CF	0.08437392	0.1231430	0.685	0.9990
	2016,CB - 2016,CP	0.19421027	0.1552311	1.251	0.9449
	2017,CB - 2018,CB	1.06569413	0.1371253	7.772	P<0.001
	2017,CB - 2017,CF	0.60283608	0.1255053	4.803	P=0.0001
	2017,CB - 2017,CP	-0.08298555	0.1689531	-0.491	0.9999
	2018,CB - 2018,CF	-0.07816741	0.1473550	-0.530	0.9998
	2018,CB - 2018,CP	-0.58274556	0.1845685	-3.157	0.0423
	2016,CF - 2017,CF	0.30444795	0.1275667	2.387	0.2912
	2016,CF - 2018,CF	0.68913859	0.1323788	5.206	P<0.001
	2016,CF - 2016,CP	0.10983636	0.1552721	0.707	0.9987
	2017,CF - 2018,CF	0.38451636	0.1350354	2.848	0.1019
	2017,CF - 2017,CP	-0.68582163	0.173978	-3.942	P<0.01
	2018,CF - 2018,CP	-0.50457815	0.1794653	-2.812	0.1118
	2016,CP - 2017,CP	-0.49121004	0.1929108	-2.546	0.2099
	2016,CP - 2018,CP	0.07472407	0.1950656	0.383	1.0000
	2017,CP - 2018,CP	0.56593412	0.2072151	2.731	0.1369
Postelsia palmaeformis	2016,CB - 2017,CB	-0.018264406	0.01467930	-.244	0.9466
	2016,CB - 2018,CB	-0.109461281	0.01530423	-7.152	P<0.001
	2016,CB - 2016,CF	-0.262666653	0.01370768	-19.162	P<0.001
	2016,CB - 2016,CP	0.029040147	0.01436294	2.022	0.5279
	2017,CB - 2018,CB	-0.091196875	0.01542647	-5.912	P<0.001
	2017,CB - 2017,CF	-0.094768137	0.01345312	-7.044	P<0.001
	2017,CB - 2017,CP	0.005502947	0.01479947	0.372	1.000
	2018,CB - 2018,CF	0.045759380	0.01372245	3.335	0.0241
	2018,CB - 2018,CP	0.174500934	0.01490530	11.707	P<0.001
	2016,CF - 2017,CF	0.149634110	0.01234153	12.124	P<0.001
	2016,CF - 2018,CF	0.198964752	0.01188596	16.739	P<0.001
	2016,CF - 2016,CP	0.291706800	0.01350535	21.599	P<0.001
	2017,CF - 2018,CF	0.049330643	0.01140565	4.325	P<0.01
	2017,CF - 2017,CP	0.100271084	0.01341400	7.475	P<0.001
	2017,CF - 2017,CP	0.100271084	0.01341400	7.475	P<0.001
	2018,CF - 2018,CP	0.128741553	0.01235962	10.416	P<0.001
	2016,CP - 2017,CP	-0.041801606	0.01447691	-2.887	0.0916
	2016,CP - 2018,CP	0.035999506	0.01391280	2.588	0.1917
	2017,CP - 2018,CP	0.077801112	0.01422269	5.470	P<0.001

Appendix V

Table 1C. Multiple comparisons of percent cover means using Tukey Contrasts.

Species	Linear Hypotheses	Estimate	Std. Error	Z value	Pr(>|z|)
Saccharina Sessilis	CF - CB == 0	1.2451	0.2622	4.749	P<0.001
	CP - CB == 0	1.3656	0.2599	5.253	P<0.001
	CP - CF == 0	0.1204	0.2005	0.601	0.818
Egregia menziesii	CF - CB == 0	-0.1567	0.1771	-0.885	0.64506
	CP - CB == 0	-0.7675	0.2589	-2.964	P<0.01
	CP - CF == 0	-0.6109	0.2605	-2.345	P<0.01
Postelsia palmaeformis	CF - CB == 0	0.26267	0.01371	19.162	P<0.001
	CP - CB == 0	-0.02904	0.01436	-2.022	0.107
	CP - CF == 0	0.029171	0.01351	-21.599	P<0.001

Appendix VI

Table 2A. Effect of year, cape and site on the length of the intertidal algae for the best-performing models. Results are from mixed effects models (GLMER) with only fixed effects presented.

Species	Parameter	Estimate	Std. Error	z-value	p-value
Saccharina Sessilis	Intercept	39.4947	1.7966	21.983	P<0.001
	Year2017	10.3554	1.6250	6.373	P<0.001
	Year2018	18.5868	1.8678	9.951	P<0.001
	MonthJune	-11.3085	0.9017	-12.542	P<0.001
	MonthMay	-19.5571	0.8385	-23.323	P<0.001
	CapeCF	-5.7967	1.1969	-4.843	P<0.001
	CapeCP	6.5416	1.5284	4.280	P<0.001
	SiteCB	-3.592	1.602	-2.242	P<0.05
	SiteFC	4.3431	1.0994	3.950	P<0.001
	SiteYB	-4.9489	1.5675	-3.157	P<0.01
	SiteRP	3.5461	1.5293	2.319	0.02041
	Year2017:CapeCF	6.5212	2.1407	3.046	P<0.01
	Year2018:CapeCF	-13.0078	2.1409	-6.076	P<0.001
	Year2017:CapeCP	-6.6693	2.3601	-2.826	0.00472
	Year2018:CapeCP	-21.1864	2.3923	-8.856	P<0.001
	Year2017:SiteFC	-10.9326	2.0530	-5.325	P<0.001
	Year2018:SiteFC	-0.8396	1.7879	-0.470	0.63865
	Year2017:SiteYB	3.0627	2.4244	1.263	0.20649
	Year2018:SiteYB	16.9127	2.4706	6.846	P<0.001
	Year2017:SiteRP	-0.3687	2.4244	1.263	0.20649
	Year2018:SiteRP	-7.4681	2.6747	-2.792	P<0.001
Egregia menziesii	Intercept	189.5133	6.0738	31.202	P<0.001
	Year2017	16.3479	7.3708	2.218	P<0.05
	Year2018	-39.7753	6.0193	-6.608	P<0.001
	CapeCF	-116.8725	6.0100	-19.446	P<0.001
	CapeCP	-111.8863	8.1039	-13.807	P<0.001
	SiteCB	-39.1310	6.8408	-5.720	P<0.001
	SiteFC	66.3317	6.0944	10.884	P<0.001
	SiteSH	36.3468	6.8887	5.276	P<0.001
	Year2017:CapeCF	-8.3046	6.4728	-1.283	0.199493
	Year2018:CapeCF	39.1108	5.8023	6.741	P<0.001
	Year2017:CapeCP	1.0860	12.4451	0.087	0.930464
	Year2018:CapeCP	17.5734	7.4808	2.349	P<0.05
	Year2017:SiteCB	0.7442	7.2320	0.103	0.918038
	Year2018:SiteCB	34.0550	9.0390	3.768	P<0.001
	Year2017:SiteFC	19.2148	8.2677	2.324	P<0.05
	Year2018:SiteFC	-2.7939	8.9663	-0.312	0.755339
	Year2017:SiteSH	32.5535	10.6804	3.048	P<0.001
	Year2018:SiteSH	56.5152	11.0094	5.133	P<0.001
Postelsia palmaeformis	Intercept	20.24261	1.03192	19.616	P<0.001
	Year2017	4.13099	1.09045	3.788	P<0.01
	Year2018	9.38129	1.25770	7.459	P<0.001
	MonthJune	-5.35270	0.60042	-8.915	P<0.001
	MonthMay	-10.92897	0.54768	-19.955	P<0.001
	CapeCF	8.14034	1.13483	7.173	P<0.001
	CapeCP	-4.87241	0.76734	-6.350	P<0.001
	SiteDB	-7.37656	1.08122	-6.822	P<0.05
	Year2017:CapeCF	-9.18213	1.64472	-5.583	P<0.001
	Year2018:CapeCF	-15.62596	1.73912	-8.985	P<0.001
	Year2017:CapeCP	-0.02498	1.27569	-0.020	0.984378
	Year2018:CapeCP	-10.22471	1.31498	-7.776	P<0.001
	Year2017:SiteCB	-0.749	2.511	-0.298	0.765524
	Year2017:SiteDB	5.84691	1.49100	3.921	P<0.001
	Year2018:SiteDB	3.24961	1.40854	2.307	0.021051

Appendix VII

Table 2B. Pairwise comparison in length post-hoc results from experimental analysis using Tukey for each species.

Species		Estimate	Std. Error	Z ratio	p.value
Saccharina Sessilis	2016,CB - 2017,CB	-10.1711100	1.3320525	-7.636	P<0.001
	2016,CB - 2018,CB	-14.8527868	1.4579383	-10.188	P<0.001
	2016,CB - 2016,CF	5.3981720	0.9868723	5.470	P<0.001
	2016,CB - 2016,CP	-2.2941175	1.1396186	-2.013	0.5341
	2017,CB - 2018,CB	-4.6816767	1.6452592	-2.856	0.1024
	2017,CB - 2017,CF	4.1589693	1.4203627	2.928	0.0821
	2017,CB - 2017,CP	2.6594562	1.4721616	1.806	0.6780
	2018,CB - 2018,CF	15.0917242	1.4442957	10.449	P<0.001
	2018,CB - 2018,CP	6.7018647	1.6059532	4.173	P<0.01
	2016,CF - 2017,CF	-11.4103128	1.0904364	-10.464	P<0.001
	2016,CF - 2018,CF	-5.1592346	0.9121407	-5.656	P<0.01
	2016,CF - 2016,CP	-7.6922895	1.0210607	-11.047	P<0.001
	2017,CF - 2018,CF	6.2510782	1.1811893	5.292	P<0.001
	2017,CF - 2017,CP	-1.4995130	1.3698839	-1.095	0.9752
	2018,CF - 2018,CP	-8.3898595	1.2800645	-6.554	P<0.001
	2016,CP - 2017,CP	-5.2175363	1.2922366	-4.038	P<0.01
	2016,CP - 2018,CP	-5.8568046	1.3301777	-4.403	P<0.01
	2017,CP - 2018,CP	-0.6392683	1.4461488	-0.442	1.0000
Egregia menziesii	2016,CB - 2017,CB	-16.720024	7.392678	-2.262	0.3657
	2016,CB - 2018,CB	22.747823	6.686870	3.402	0.0193
	2016,CB - 2016,CF	64.141224	6.029356	10.638	P<0.001
	2016,CB - 2016,CP	74.147391	6.895442	10.753	P<0.001
	2017,CB - 2018,CB	39.467848	8.056738	4.899	P<0.001
	2017,CB - 2017,CF	63.210557	7.529464	8.395	P<0.001
	2017,CB - 2017,CP	57.156747	8.728858	6.548	P<0.001
	2018,CB - 2018,CF	43.454911	7.333197	5.926	P<0.001
	2018,CB - 2018,CP	45.343913	7.823817	5.796	P<0.001
	2016,CF - 2017,CF	-17.650691	5.989608	-2.947	0.0780
	2016,CF - 2018,CF	2.061510	5.422791	0.380	1.0000
	2016,CF - 2016,CP	10.006167	5.975183	1.675	0.7623
	2017,CF - 2018,CF	19.712202	6.544232	3.012	0.0649
	2017,CF - 2017,CP	-6.053809	8.685269	-0.697	0.9988
	2018,CF - 2018,CP	1.889002	6.848217	0.276	1.0000
	2016,CP - 2017,CP	-33.710668	8.309893	-4.057	0.0016
	2016,CP - 2018,CP	-6.055655	6.605632	-0.917	0.9921
	2017,CP - 2018,CP	27.655013	8.803448	3.141	0.0444
Postelsia palmaeformis	2016,CB - 2017,CB	-4.1309942	1.0904486	-3.788	0.0048
	2016,CB - 2018,CB	-9.3812919	1.2577023	-7.459	P<0.001
	2016,CB - 2016,CF	-4.4520537	0.8711418	-5.111	P<0.001
	2016,CB - 2016,CP	4.8724098	0.7673382	6.350	P<0.001
	2017,CB - 2018,CB	-5.2502976	1.3633476	-3.851	0.0038
	2017,CB - 2017,CF	1.8066229	1.0024924	1.802	0.6809
	2017,CB - 2017,CP	4.8973889	1.0430659	4.695	P=0.001
	2018,CB - 2018,CF	9.5491000	1.1629192	8.211	P<0.001
	2018,CB -2018,CP	15.0971160	1.1158062	13.530	P<0.001
	2016,CF - 2017,CF	2.1276823	0.752691	2.827	0.1075
	2016,CF - 2018,CF	4.6198618	0.7132523	6.477	P<0.001
	2016,CF - 2016,CP	9.3244635	0.6402933	14.563	P<0.001
	2017,CF - 2018,CF	2.4921795	0.6972797	3.574	0.0106
	2017,CF - 2017,CP	3.0907660	0.7923065	3.901	0.0031
	2018,CF - 2018,CP	5.5480160	0.5494942	10.097	P<0.001
	2016,CP - 2017,CP	-4.1060151	0.6622583	-6.200	P<0.001
	2016,CP - 2018,CP	0.8434143	0.3872872	2.178	0.4203
	2017,CP - 2018,CP	4.9494294	0.6468130	7.652	P<0.001

Appendix VIII

Table 3. Pearson correlation between environmental parameters and biological responses. The strongest linear relationship is indicated by a correlation coefficient of -1 or 1. The weakest linear relationship is indicated by a correlation coefficient equal to 0. The correlations with p-value> 0.01 are considered as insignificant and are left blank.

Factors	Cover	Density	Length	Chl a	DIN	SST	MEI	NPGO	PDO	Upwelling	SWVHT	
												Cover
	0.63											**Density**
	0.39	0.11										**Length**
	-0.09	-0.27	0.15									**Chl a**
	0.19	0.1	0.17	0.08								**DIN**
	-0.05	0.18	-0.16	-0.17	-0.45							**SST**
	-0.36	-0.003	-0.43	-0.39		0.37						**MEI**
	0.34	0.004	0.42	0.31	-0.17	-0.2	-0.97					**NPGO**
	-0.33		-0.37	-0.48	-0.34	0.67	0.85	0.71				**PDO**
	0.32		0.36	0.48	0.37	-0.69	-0.82	0.67	-1.00			**Upwelling**
	-0.34		-0.39	-0.47	-0.27	0.62	0.91	-0.78	0.99	-0.99		**SSWHT**

AGRO CAMPUS OUEST	Diplôme : Ingénieur Spécialité : Agronome Spécialisation / option : Sciences Halieutiques et Aquacoles – option REA Enseignant référent : Olivier Le Pape

Auteur(s) : Camille Ollier Date de naissance : 04/12/1994	Organisme d'accueil : Oregon State University Adresse : Department of Integrative Biology 3029 Cordley Hall 2701 SW Campus Way OR 97331 Corvallis, United States, Maître de stage : Bruce Menge; Barbara Spiecker
Nb pages : 41 Annexe(s) : 8	
Année de soutenance : 2018	

Titre français : L'influence des processus océanographiques locaux et régionaux sur la restauration des communautés de macroalgues post-El Niño sur les zones intertidales rocheuses côtières de l'Oregon

Titre anglais : Effect of local and regional oceanographic processes on the recovery of macroalgal communities post-El Niño in the rocky intertidal along the Oregon coast

Résumé : Bien que les liens entre le changement climatique et les signaux climatiques comme ENSO (*El Niño-Southern Oscillation*) soient encore flous, les effets à court terme des événements ENSO sur les environnements côtiers semblent imiter ceux à long terme du changement climatique. De ce fait, ENSO peut être utilisé comme indicateur des réponses écologiques possibles à long terme à un climat aux variations accrues. Les événements ENSO peuvent avoir des effets majeurs sur les interactions des espèces et sur la structuration des communautés. Cependant, l'impact d'El Niño pourrait être modulé par les processus locaux et régionaux (apports de nutriments via les remontées d'eau, topographie côtière, etc.). Les zones intertidales de l'Oregon sont exposées à un gradient de remontées allant de faible/intermédiaire (nord) à fort/persistant (sud), et la topographie côtière varie entre les sites. Les résultats ont montré que les processus environnementaux locaux et régionaux y modulent de fait les effets d'El Niño sur la restauration des communautés de varech. L'abondance et la taille de celles-ci ont été réduites par El Niño 2015-16 (plus fort au sud) et se sont restaurées deux ans après, avec un rythme supérieur au sud. Selon les résultats, les processus climatiques persistants à grande échelle (p. ex. réchauffement) pourraient s'avérer délétères pour les relations bénéfiques entre remontées d'eau et communautés. Il faudra des recherches à plus grande échelle spatiale et temporelle pour mieux comprendre et anticiper les impacts du changement climatique sur ces communautés.

Abstract: Although the links between climate change and climatic patterns such as ENSO (El Niño-Southern Oscillation) remain unclear, the impacts of ENSO events on coastal environments in the short-term likely mimic those of climate change in the long-term. Thus, ENSO can serve as a proxy for possible long-term ecological responses to an increasingly variable climate. ENSO events can have dramatic effects on species interactions and the structuring of communities. However, the impact of El Niño could be modulated by local and regional processes (i.e., nutrient inputs from upwelling and coastal topography). The Oregon rocky intertidal is exposed to a gradient of upwelling from weaker and intermediate (northern Oregon) to stronger and more persistent (southern Oregon) and the coastal topography varies from site to site. The results showed that local and regional environmental processes do modulate the strength of El Niño and its effects on the recovery of kelp communities along the Oregon coast. Intertidal kelp abundance and size were reduced by the 2015-16 El Niño event (more so in the southern Oregon) and they were recovered two years after the event with a faster recovery rate in the southern Oregon. The results hint at the possibility of persistent large-scale climatic processes (i.e., warming) shifting the beneficial relationship between upwelling and kelp communities to a harmful one. More research is needed on larger spatial and temporal scales to better understand and anticipate future climate change ramifications on the intertidal kelp communities.

Mots-clés : Varech intertidal, El Niño, Upwelling, Changement climatique

Key Words: Intertidal kelp, El Niño, Upwelling, Climate change